Stony Brook University | The State University of New York

Wave Gradiometry and Helmholtz Solution Correction Applied to USArray

William Holt, Yuanyuan Liu, Ryan Porter, Hejun Zhu

NSF

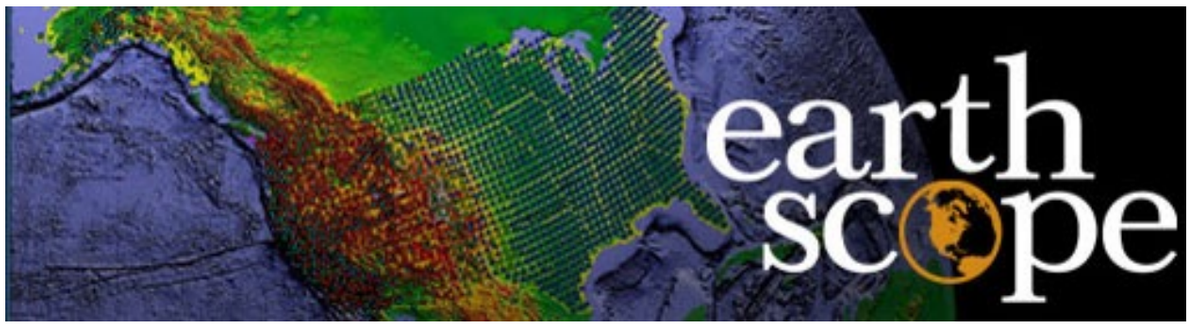

IRIS

UNAVCO

SCEC
an NSF + USGS center

Outline

- Introduction and Motivation
- Wave Gradiometry and its Link with Helmholtz Equation Solution
- Analysis of Six Events in Gulf of California
- Analysis of Rayleigh Wave Isotropic Structural Phase velocity
- Inversion for Shear Velocity Models across the Continental U.S.
- Discussion and Conclusion

Outline

- **Introduction and Motivation**
- Wave Gradiometry and its Link with Helmholtz Equation Solution
- Analysis of Six Events in Gulf of California
- Analysis of Rayleigh Wave Isotropic Structural Phase velocity
- Inversion for Shear Velocity Models across the Continental U.S.
- Discussion and Conclusion

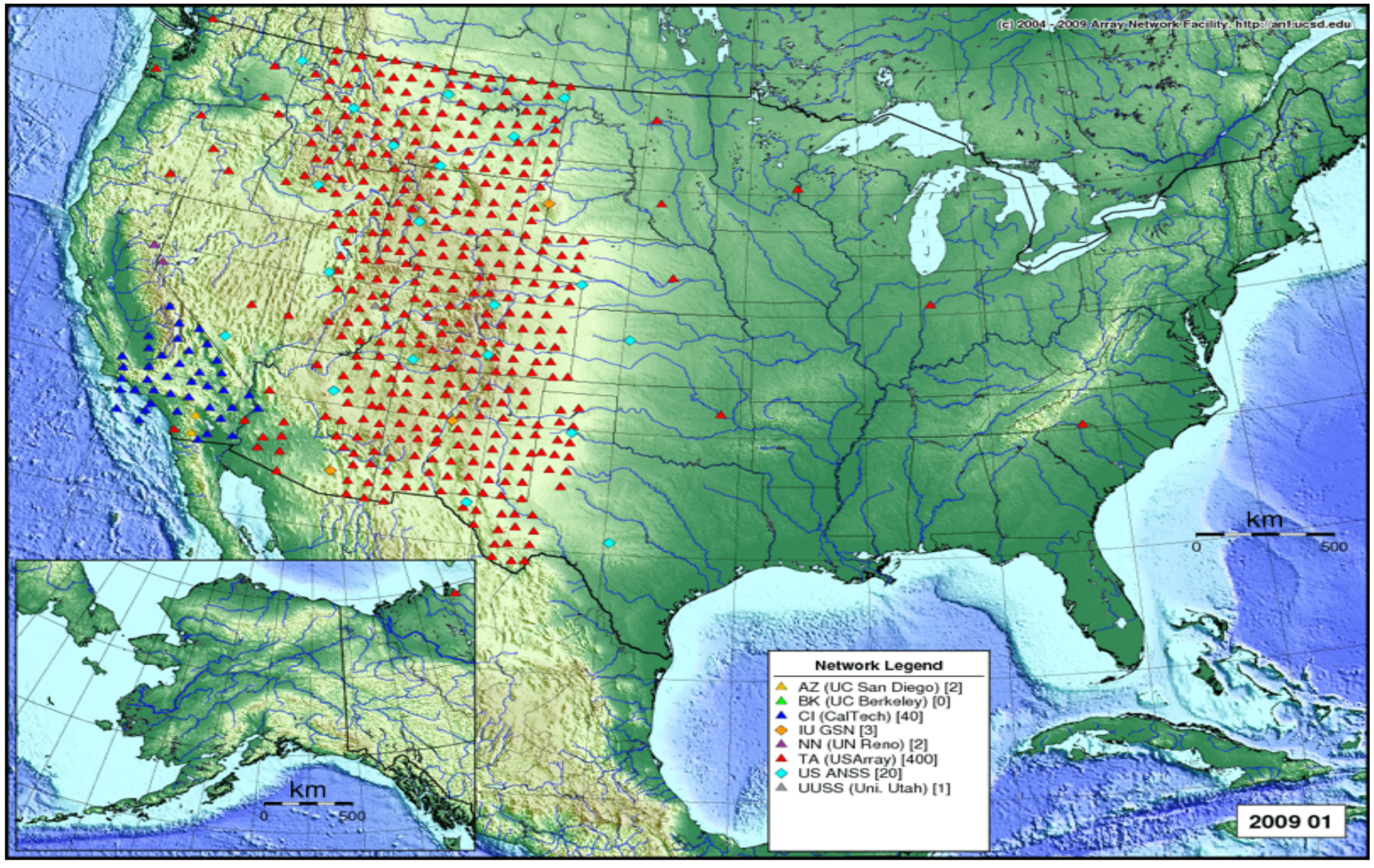

The USArray Transportable Array is a network of 400 high-quality broadband seismometers that are being placed in temporary sites across the United States from west to east, in a regular grid pattern.

From http://anf.ucsd.edu/stations.php

Displacements + Contoured Dilatational Strains

Principal Strain Axes + Contoured Shear Strains

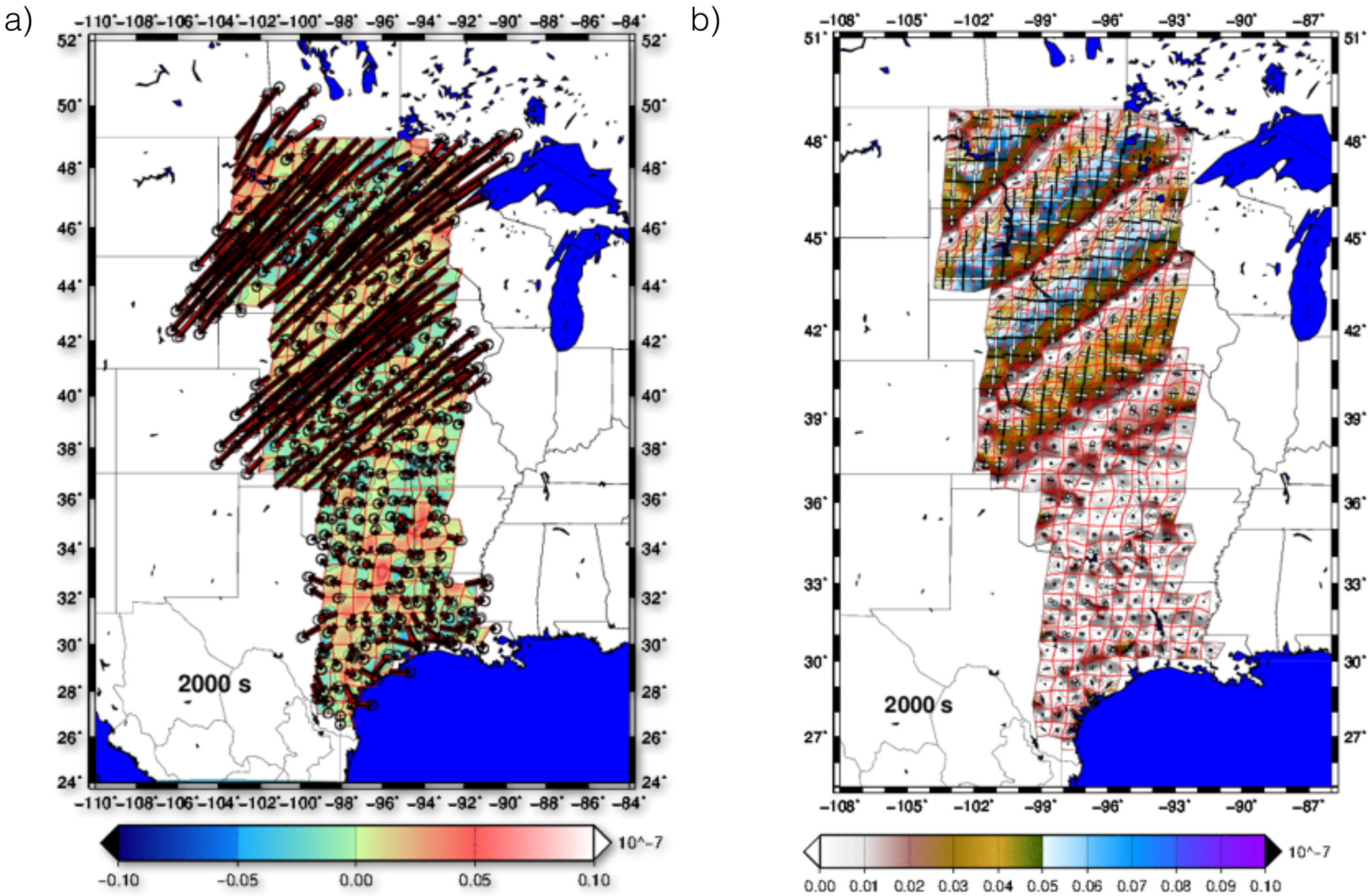

(a) Horizontal components of surface waves from 2011 Great Japan Earthquake. Red vector is observed horizontal displacement and the black vector is the model field predicted by the bi-cubic spline interpolation of the displacement field.
(b) Principal axes of strain with contoured shear strain rate (pure strike-slip style)

Outline

- Introduction and Motivation
- **Wave Gradiometry and its Link with Helmholtz Equation Solution**
- Analysis of Six Events in Gulf of California
- Analysis of Rayleigh Wave Isotropic Structural Phase velocity
- Inversion for Shear Velocity Models across the Continental U.S.
- Discussion and Conclusion

a)

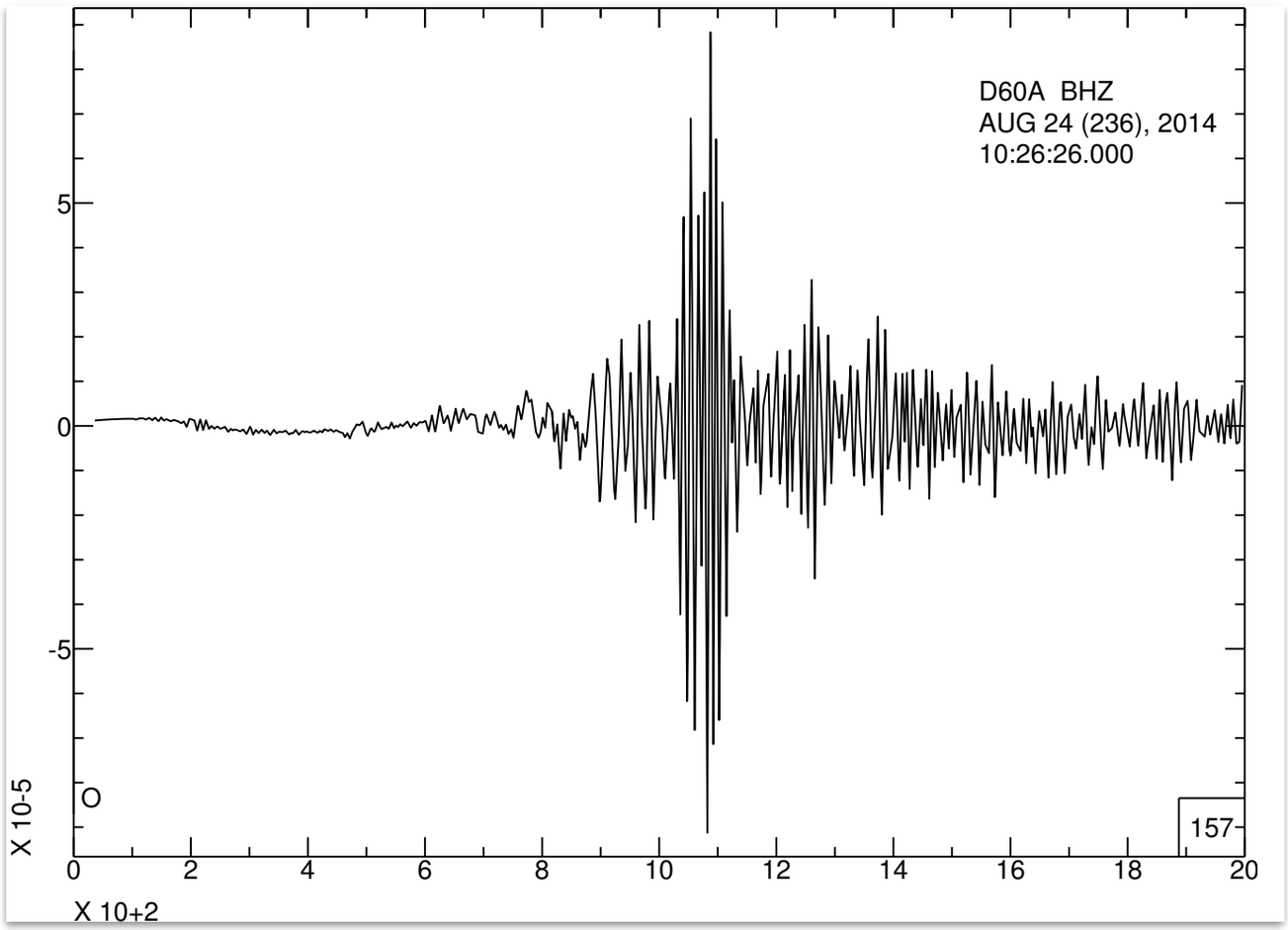

b)

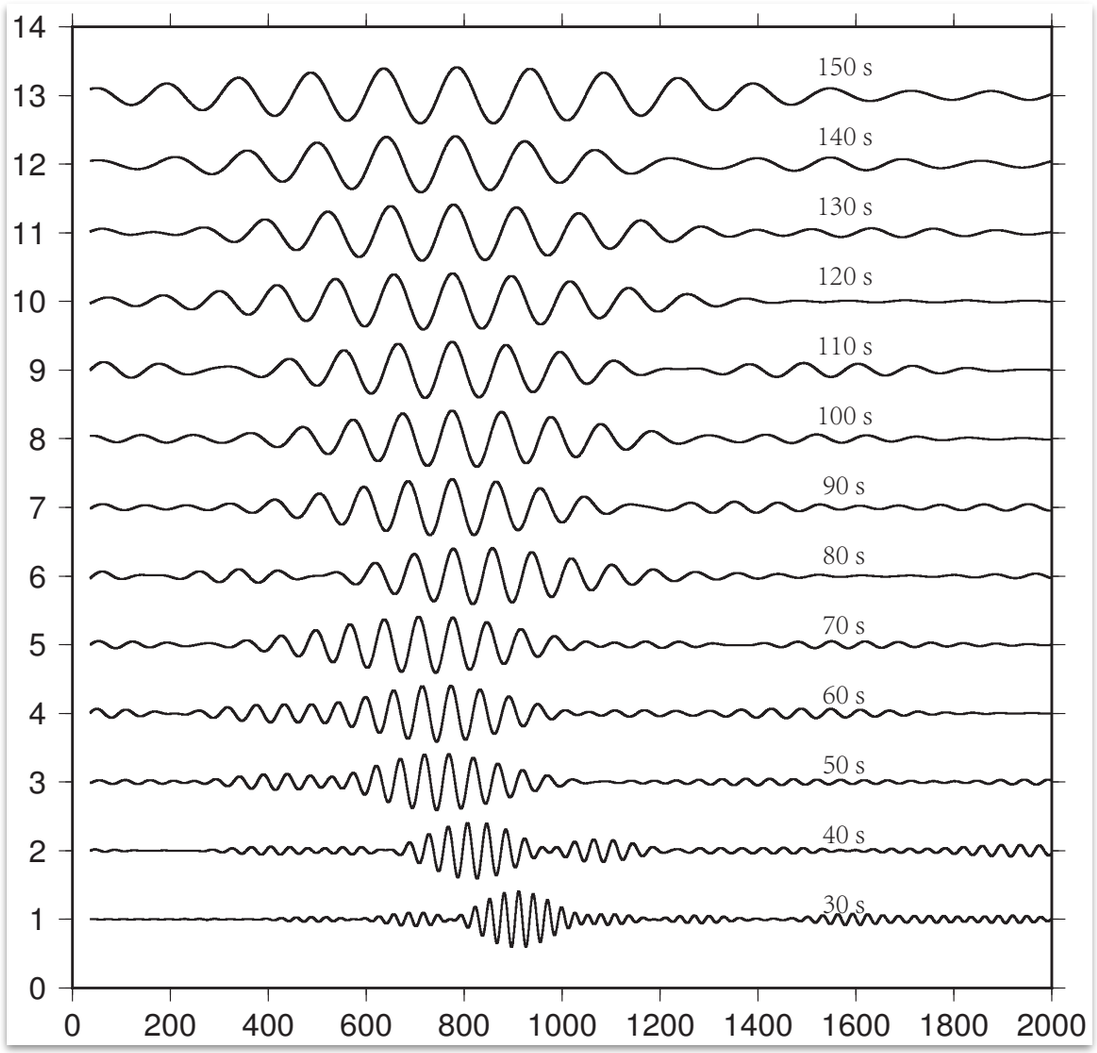

(a) Vertical component of raw waveform recorded by USArray Transportable station D60A for 2014 August 24, earthquake near northern California.

(b) The 30 s - 150 s Rayleigh waveforms after applying band-pass filters to the raw waveform in (a). We can see that the wavelength is getting longer for long periods and the Rayleigh wave phase velocity is frequency dependent.

$$u(t,r,\theta) = G(r)R(\theta)f\left\{t - p(r)\left[r - r_0\right]\right\}$$

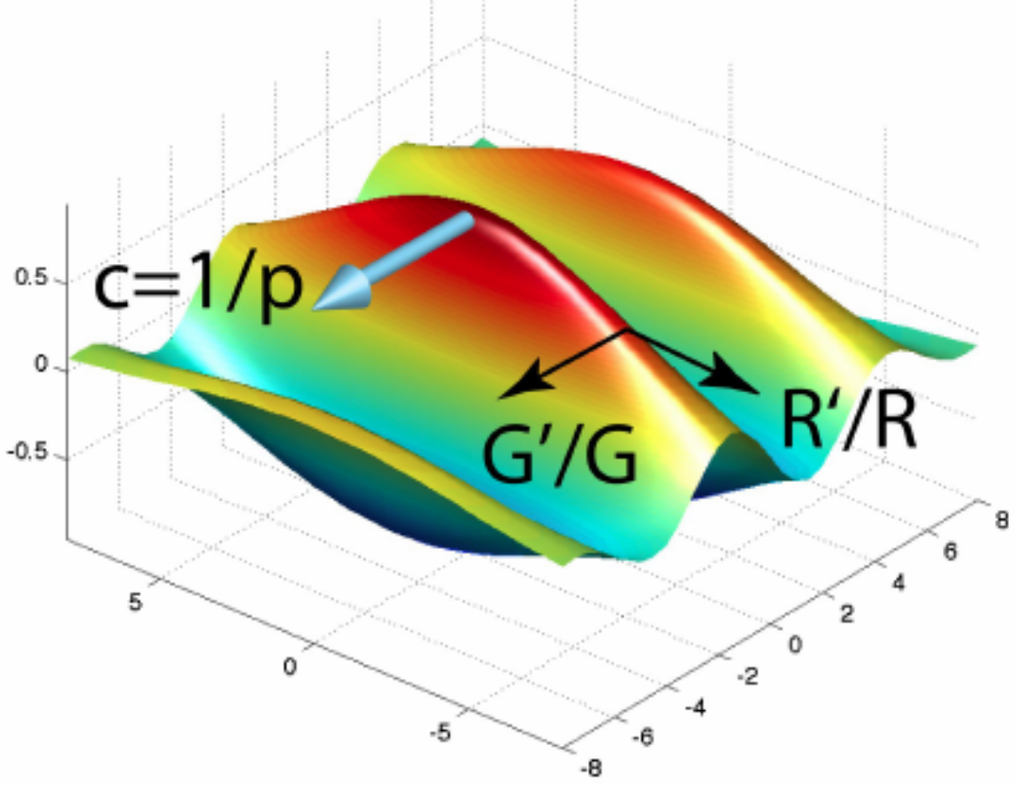

$$u_{i,j} = A_j u + B_j \dot{u}$$

G'/G & R'/R

$-p_j$

$$p_r = \sqrt{p_x^2 + p_y^2}$$

$$\tan\theta = \frac{p_x}{p_y}$$

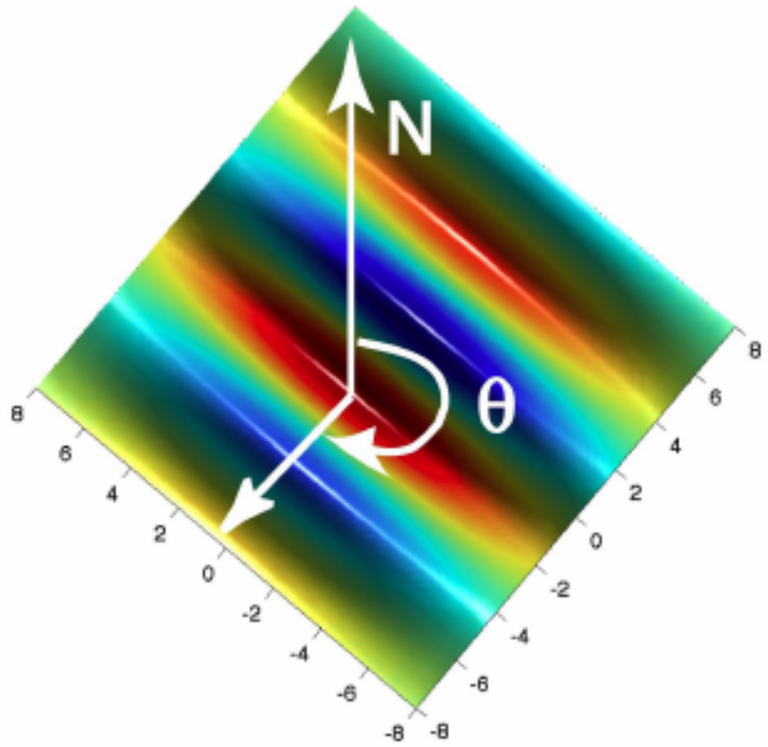

After Langston [2013]

See Langston [2007a, b, c] BSSA

Displacement gradients are determined using interpolation method of Haines and Holt [1993] and Beavan and Haines [2001]

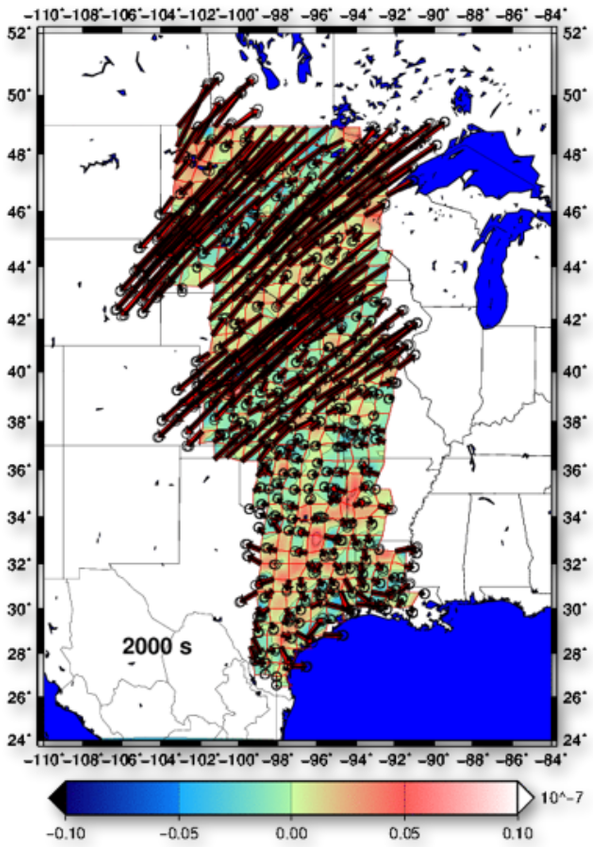

$$\mathbf{u}(\hat{\mathbf{r}}) = r\mathbf{W}(\hat{\mathbf{r}}) \times \hat{\mathbf{r}}$$

$$\varepsilon_{\phi\phi} = \frac{1}{\cos\theta}\frac{\partial u_\phi}{\partial \phi} - u_\theta \tan\theta + \frac{u_r}{r}$$

$$\varepsilon_{\theta\theta} = \frac{\partial u_\theta}{\partial \theta} + \frac{u_r}{r}$$

$$\varepsilon_{\theta\phi} = \frac{1}{2}\left[\frac{\partial u_\phi}{\partial \theta} + \frac{1}{\cos\theta}\frac{\partial u_\theta}{\partial \phi} + u_\phi \tan\theta\right]$$

$$\omega_r = \hat{\mathbf{r}} \cdot (\nabla \times \mathbf{U})$$

Strains and rotations are expressed in terms of derivatives of continuous rotation vector function **W**, defined using bi-cubic spline basis functions. Equivalent to finite-element approach with higher-order elements.

Once spatial gradients are determined, we perform iterative least-squares inversion for A and B coefficients

$$\begin{bmatrix} u|_{t_1} & \frac{\partial u}{\partial t}|_{t_1} \\ \vdots & \vdots \\ u|_{t_{101}} & \frac{\partial u}{\partial t}|_{t_{101}} \end{bmatrix} \times \begin{bmatrix} A_x \\ B_x \end{bmatrix} = \begin{bmatrix} \frac{\partial u}{\partial x}|_{t_1} \\ \vdots \\ \frac{\partial u}{\partial x}|_{t_{101}} \end{bmatrix} \quad \begin{bmatrix} u|_{t_1} & \frac{\partial u}{\partial t}|_{t_1} \\ \vdots & \vdots \\ u|_{t_{101}} & \frac{\partial u}{\partial t}|_{t_{101}} \end{bmatrix} \times \begin{bmatrix} A_y \\ B_y \end{bmatrix} = \begin{bmatrix} \frac{\partial u}{\partial y}|_{t_1} \\ \vdots \\ \frac{\partial u}{\partial y}|_{t_{101}} \end{bmatrix}$$

Reducing Velocity Method of *Liang and Langston* [2009]

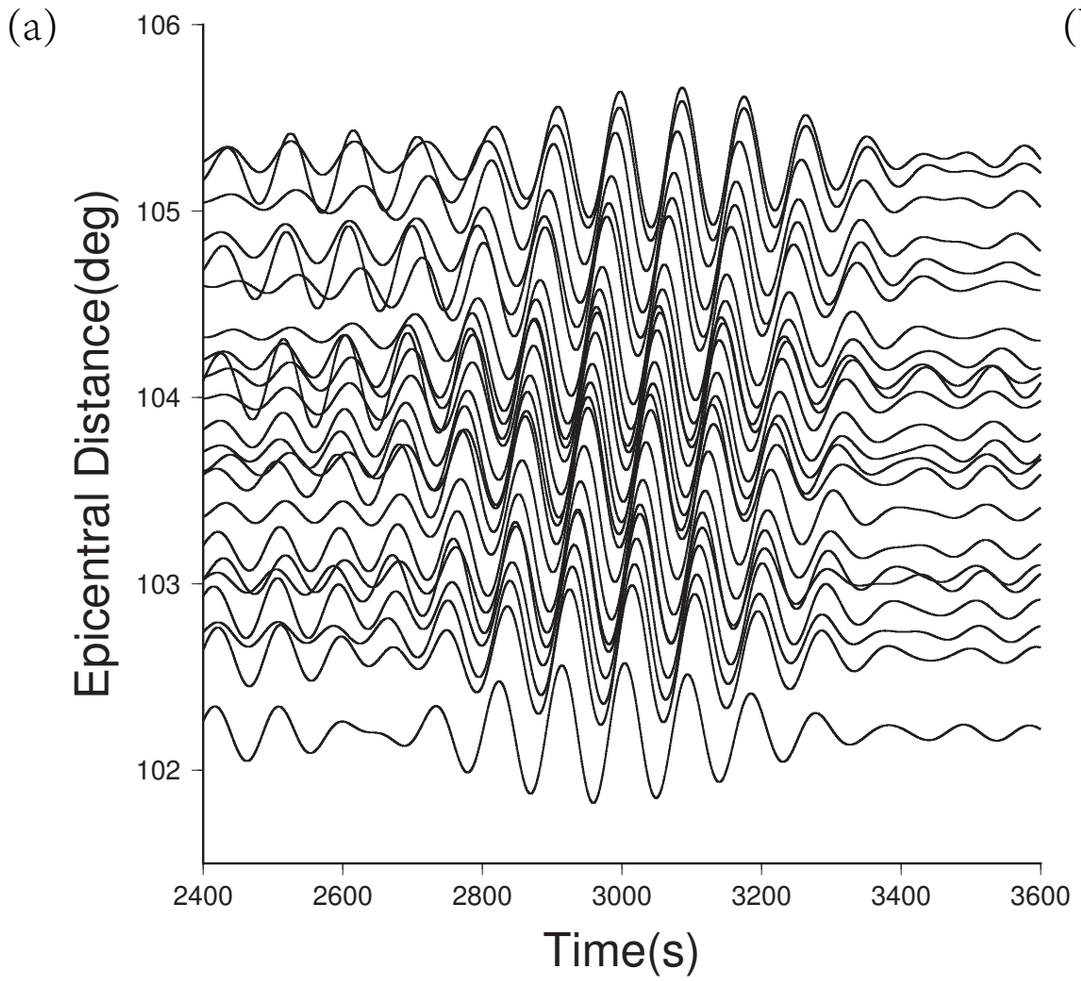

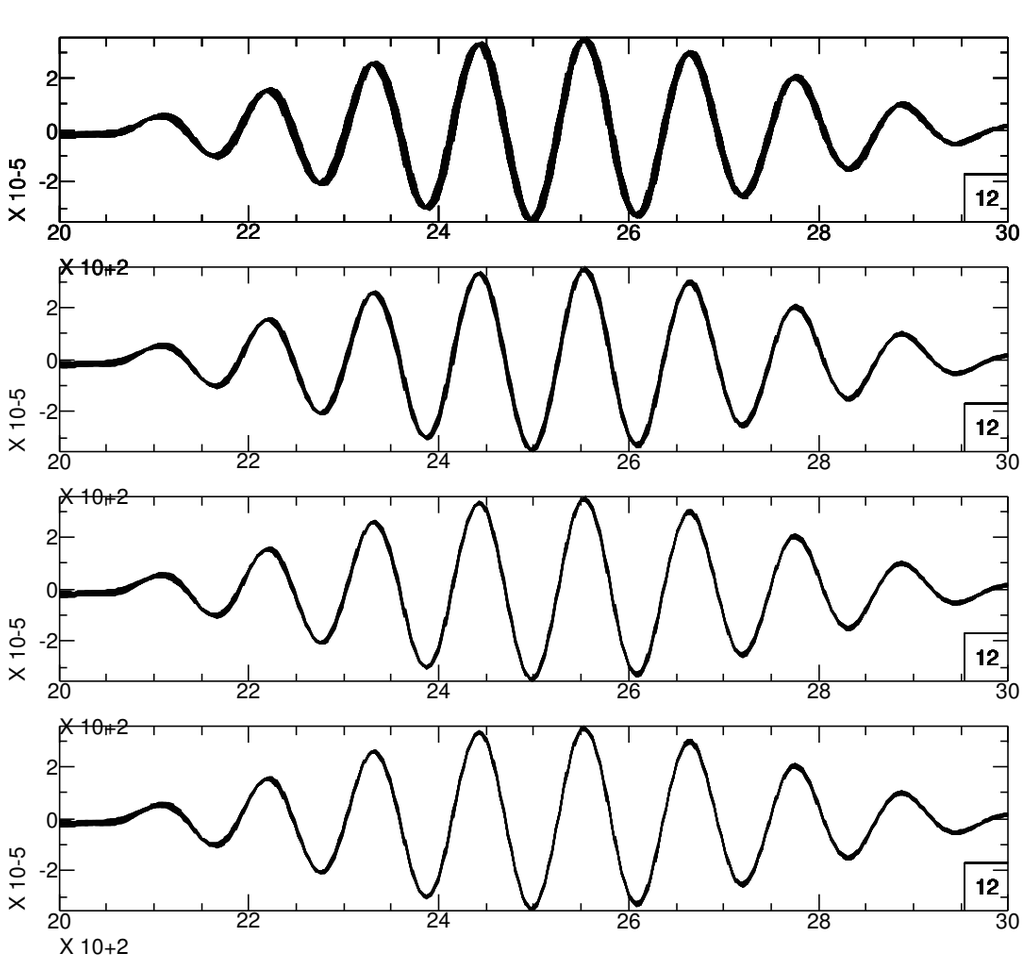

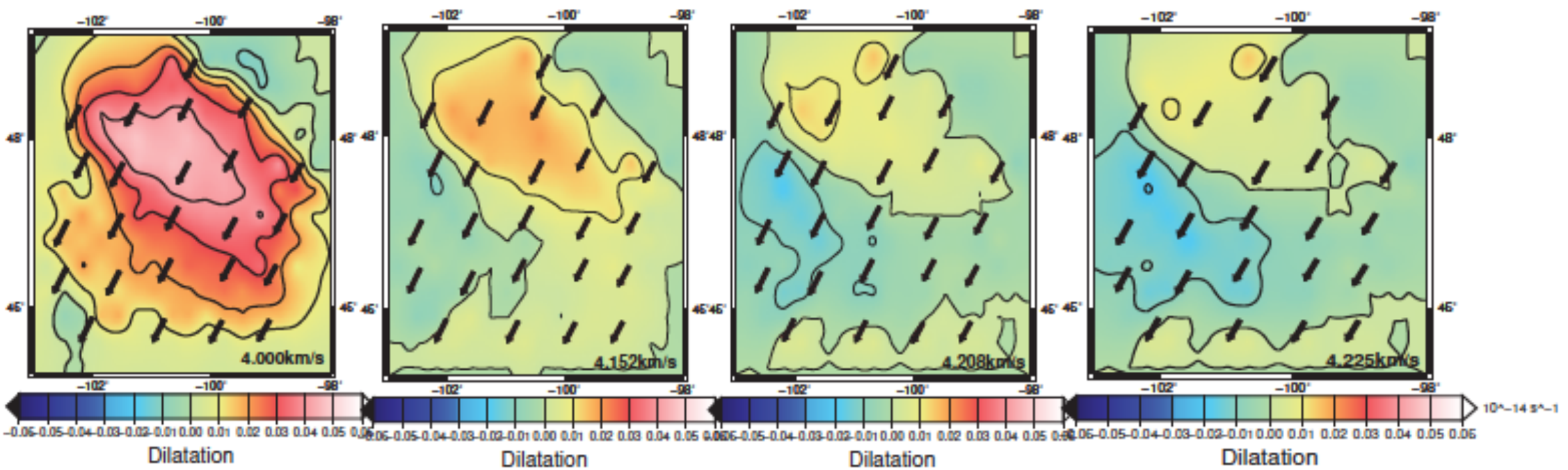

Observed and predicted straingrams

$$u_{i,j} = A_j u + B_j \dot{u}$$

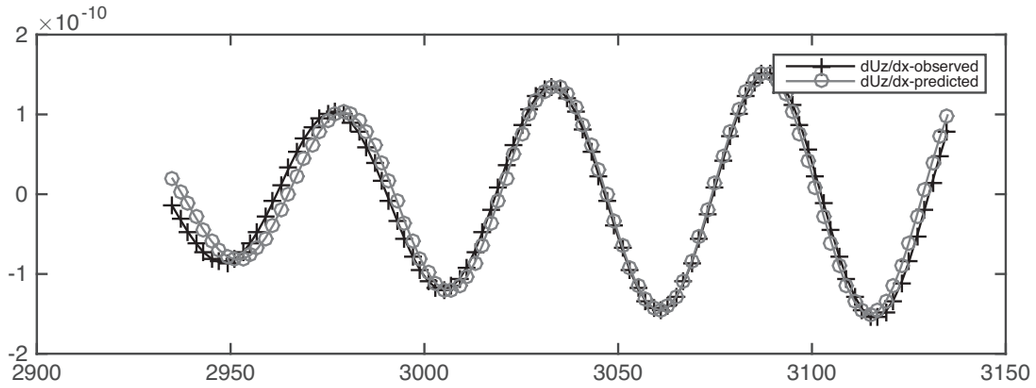

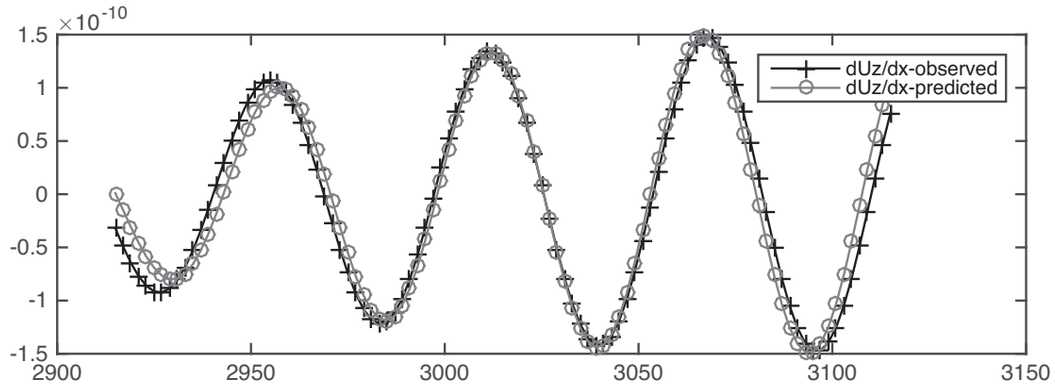

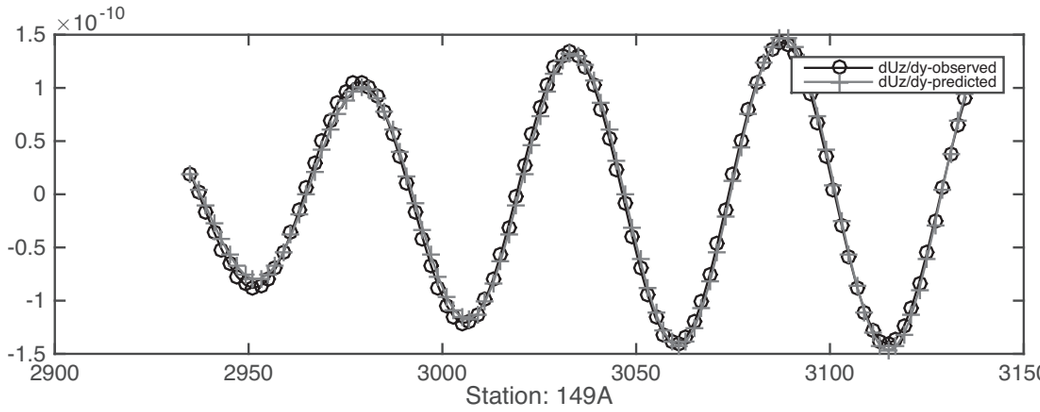

Station: 149A

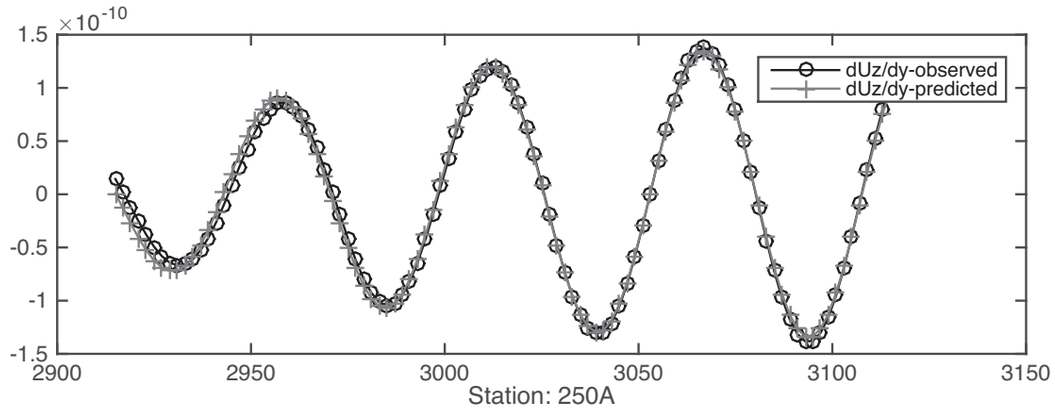

Station: 250A

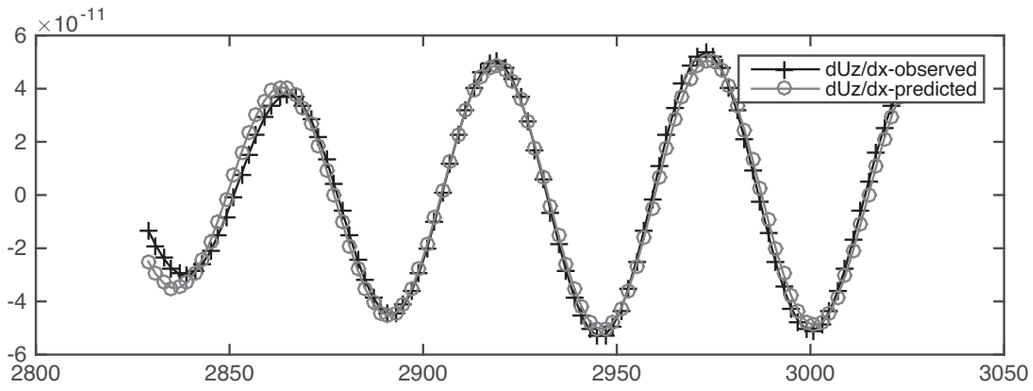

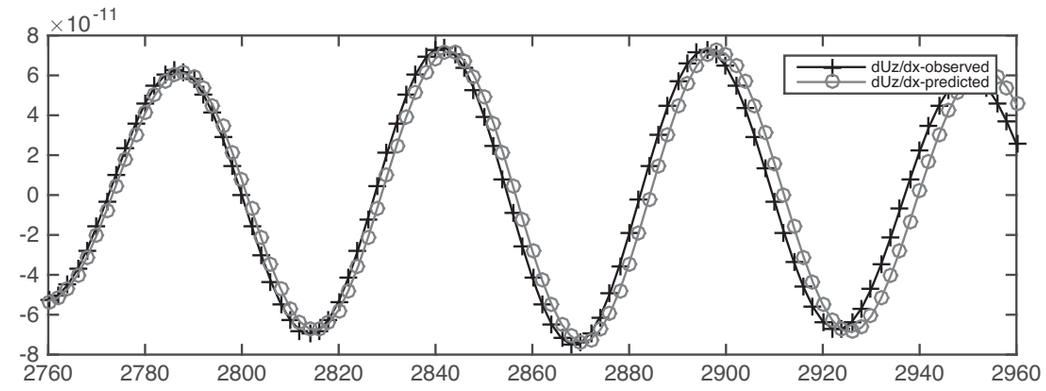

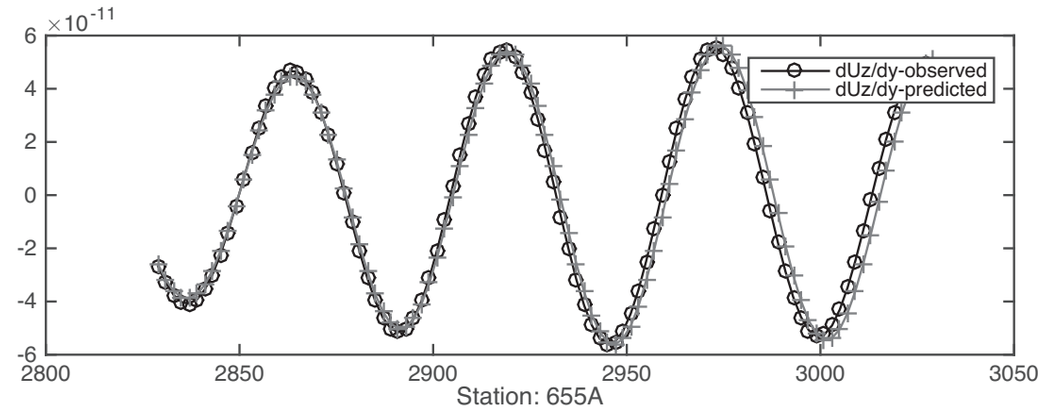

Station: 655A

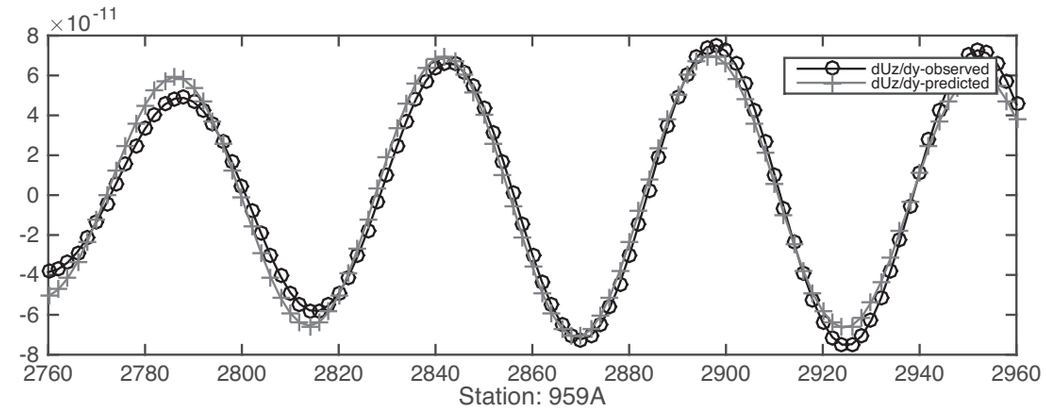

Station: 959A

Wave equation solution

$$u(x,y) = G(x,y)f(t - xp_x - yp_y)$$

$$\frac{\partial u(t,x,y)}{\partial x} = A_x \cdot u(t,x,y) + B_x \cdot \frac{\partial u(t,x,y)}{\partial t}$$

$$\frac{\partial u(t,x,y)}{\partial y} = A_y \cdot u(t,x,y) + B_y \cdot \frac{\partial u(t,x,y)}{\partial t}$$

Solved parameters

$$A_x = \frac{\partial G}{\partial x} \cdot \frac{1}{G} \qquad A_y = \frac{\partial G}{\partial y} \cdot \frac{1}{G}$$

$$B_x = -p_x \qquad B_y = -p_y$$

$$p = \sqrt{(B_x^2 + B_y^2)} \qquad A_\theta(\theta) = r(A_x cos\theta - A_y sin\theta)$$

$$\theta = tan^{-1}(\frac{B_x}{B_y}) \qquad A_r(\theta) = A_x sin\theta + A_y cos\theta$$

Helmholtz equation

$$(\Delta + k^2)F(x,y) = 0 \qquad \Delta = \frac{\partial}{\partial x^2} + \frac{\partial}{\partial y^2}$$

$$k^2 = (B \cdot \omega)^2 - A^2 - grad(A)$$

$$2 \cdot B \cdot A - grad(B) = 0$$

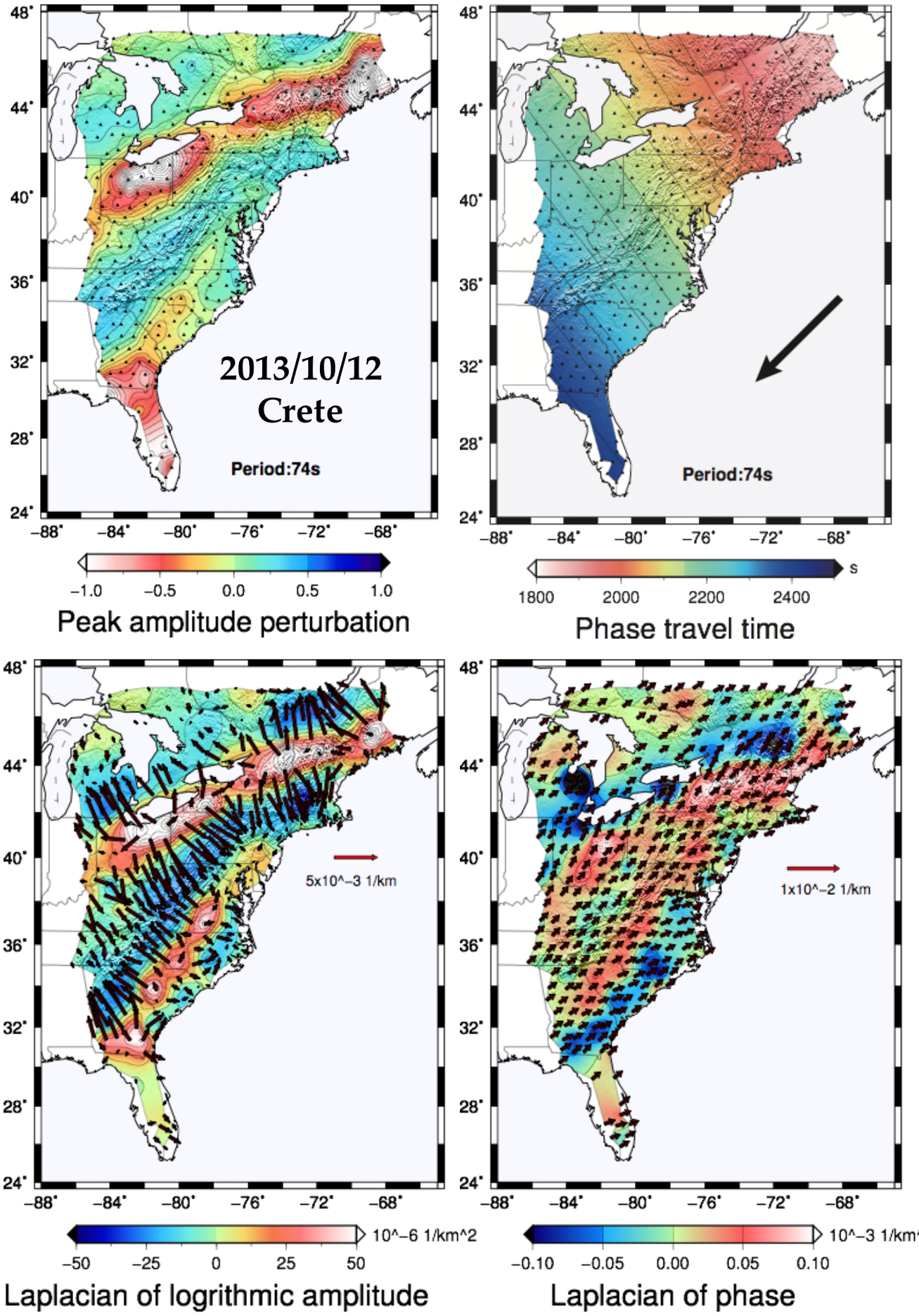

$$A_\theta(\theta) = \frac{\partial G}{\partial \theta} \cdot \frac{1}{G} = r(A_x cos\theta - A_y sin\theta)$$

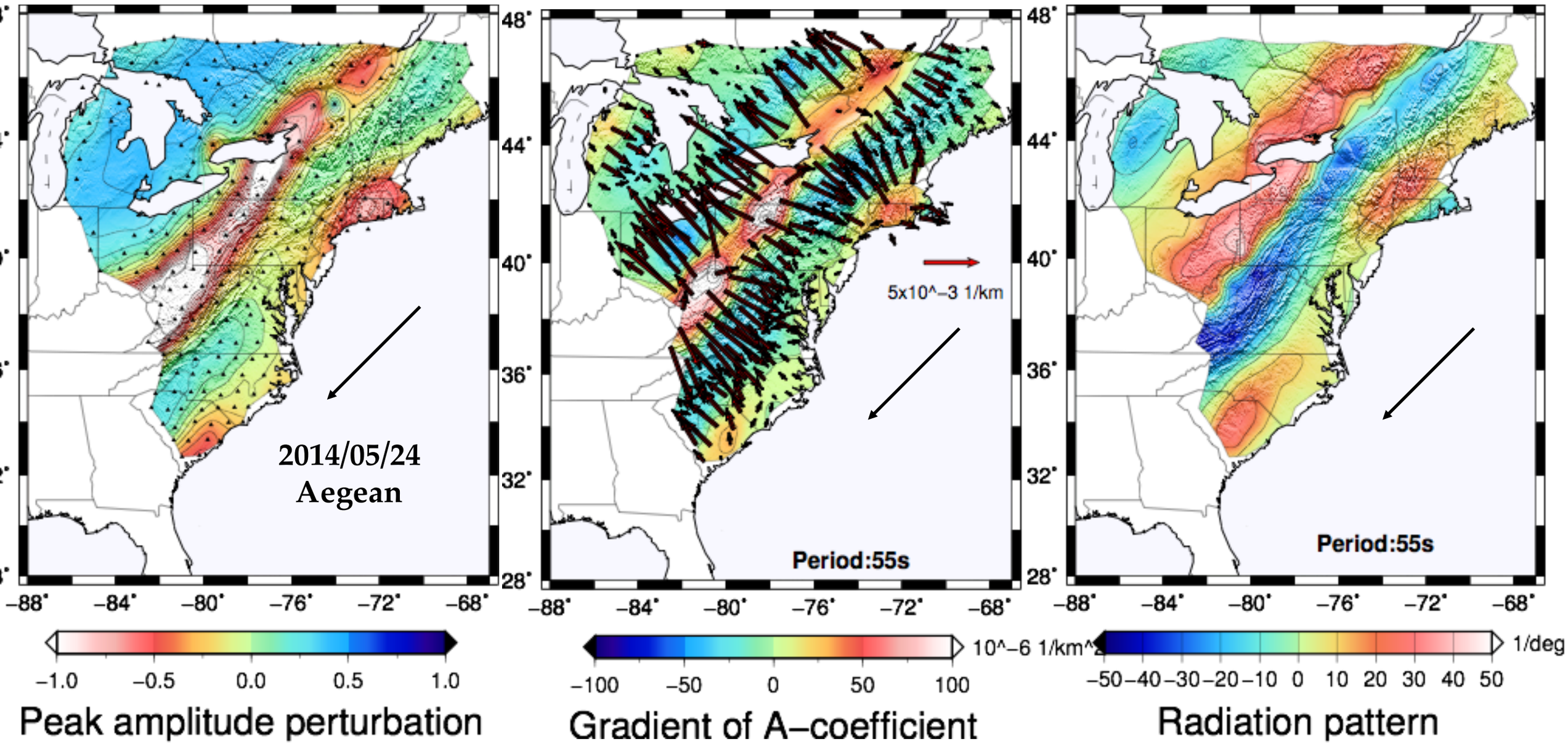

Liu and Holt, 2015, JGR

$$A_r(\theta) = \frac{\partial G}{\partial r} \cdot \frac{1}{G} = A_x sin\theta + A_y cos\theta$$

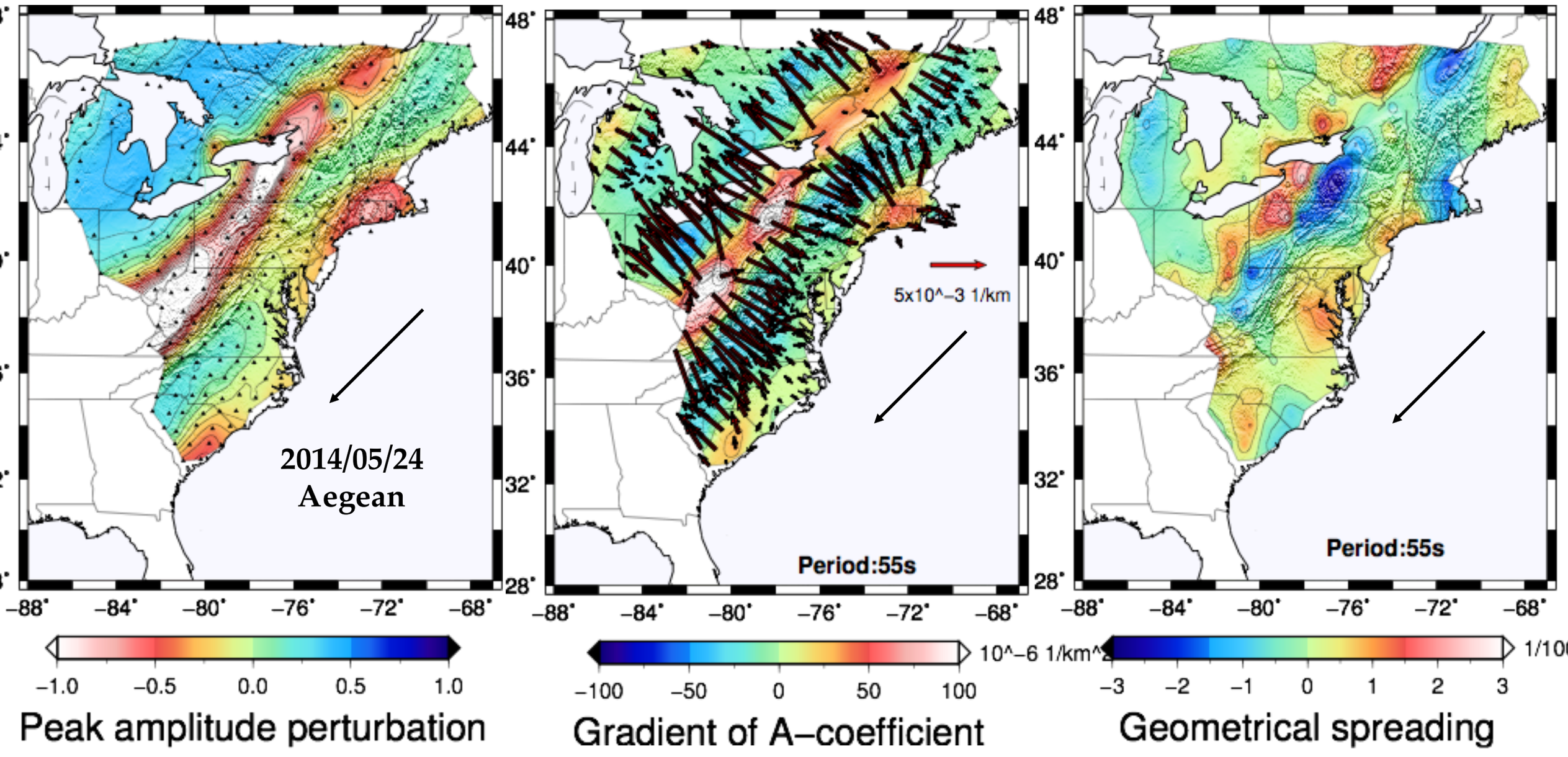

Liu and Holt, 2015, JGR

$$k^2 = (B \cdot \omega)^2 - A^2 - grad(A)$$

‘Amplitude Correction Term’
Wielandt [1993]

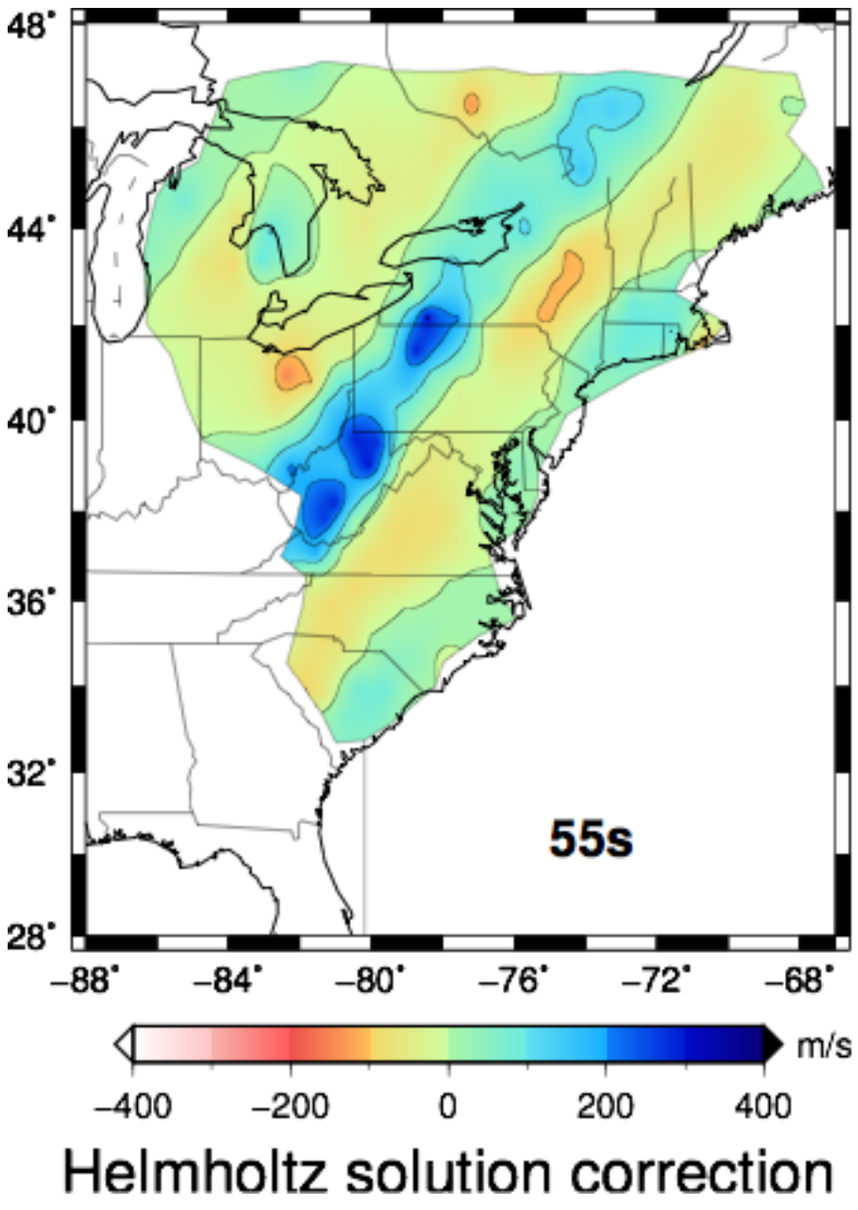

Helmholtz solution correction

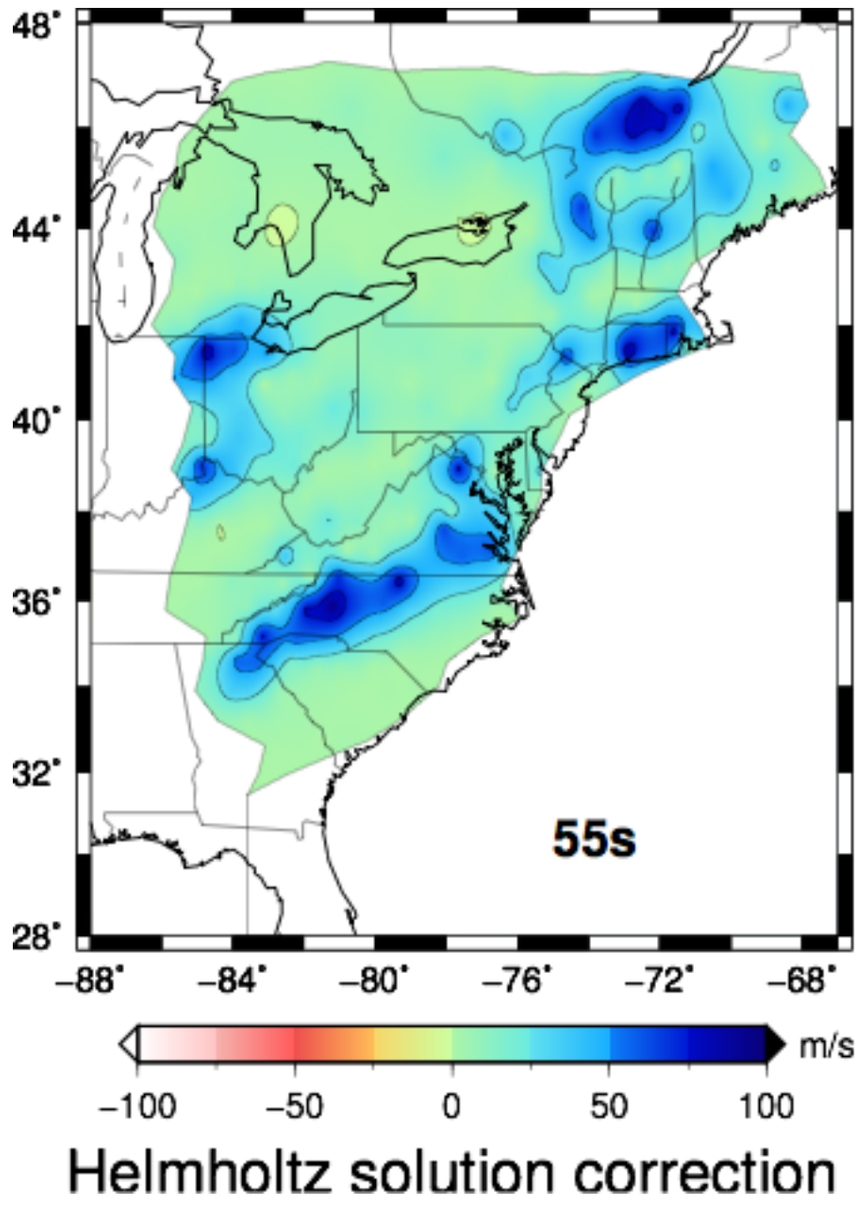

Helmholtz solution correction

$$2 \cdot \|\mathbf{B}\| \cdot \|\mathbf{A}\| \cdot cos\theta - \boxed{grad(B)} = 0$$

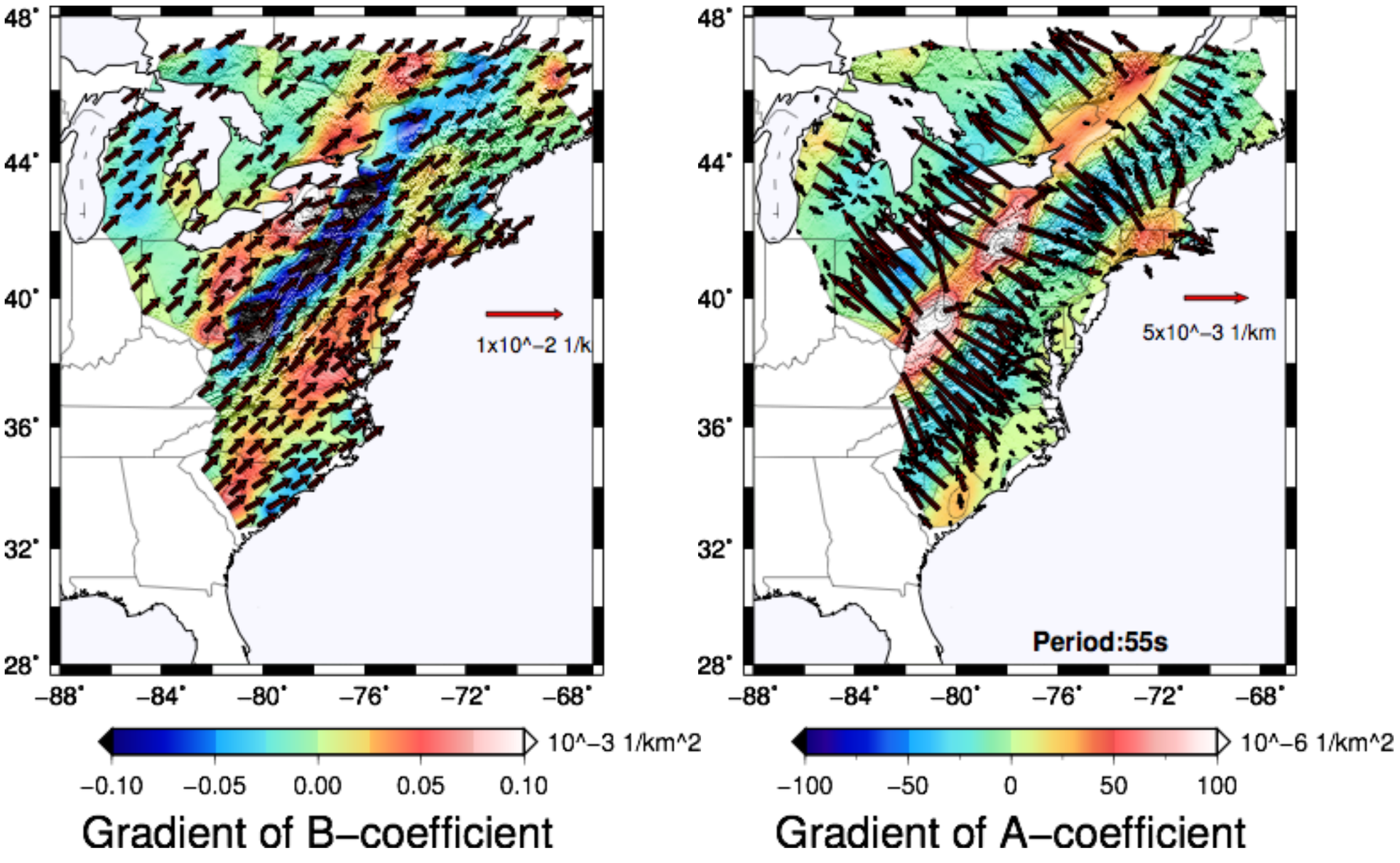

Liu and Holt, 2015, JGR

Insights into wavefield focusing and defocusing

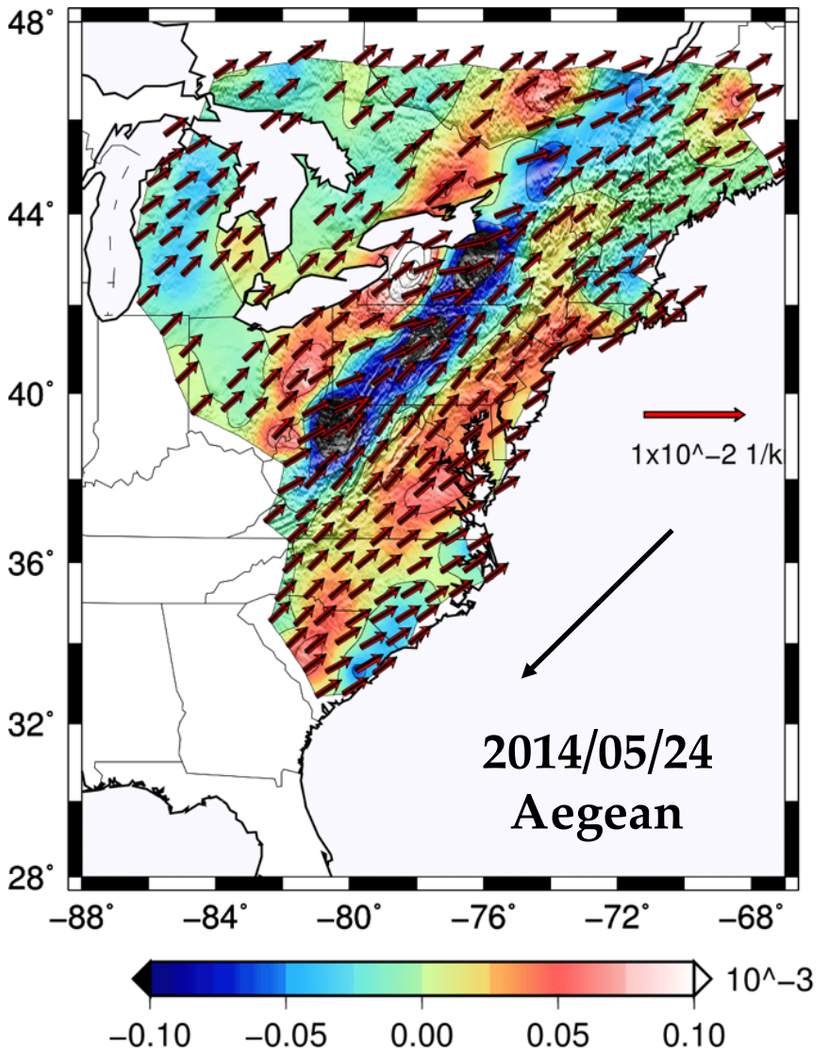

Gradient of B−coefficient

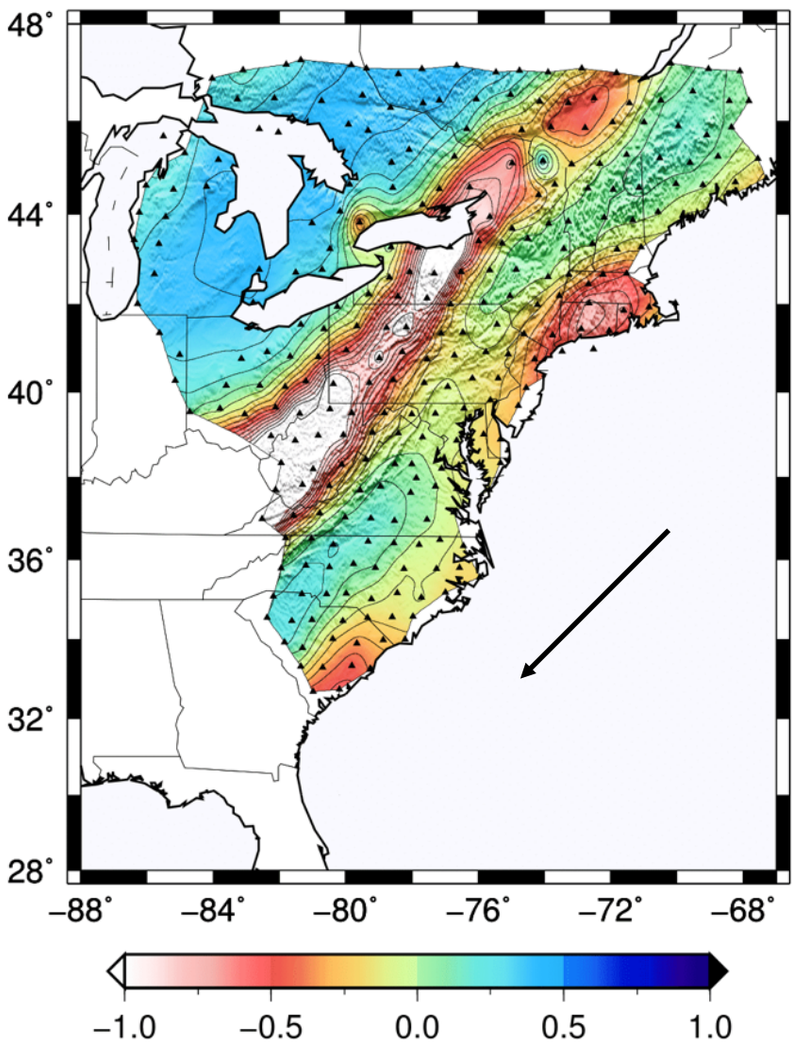

Peak amplitude perturbation

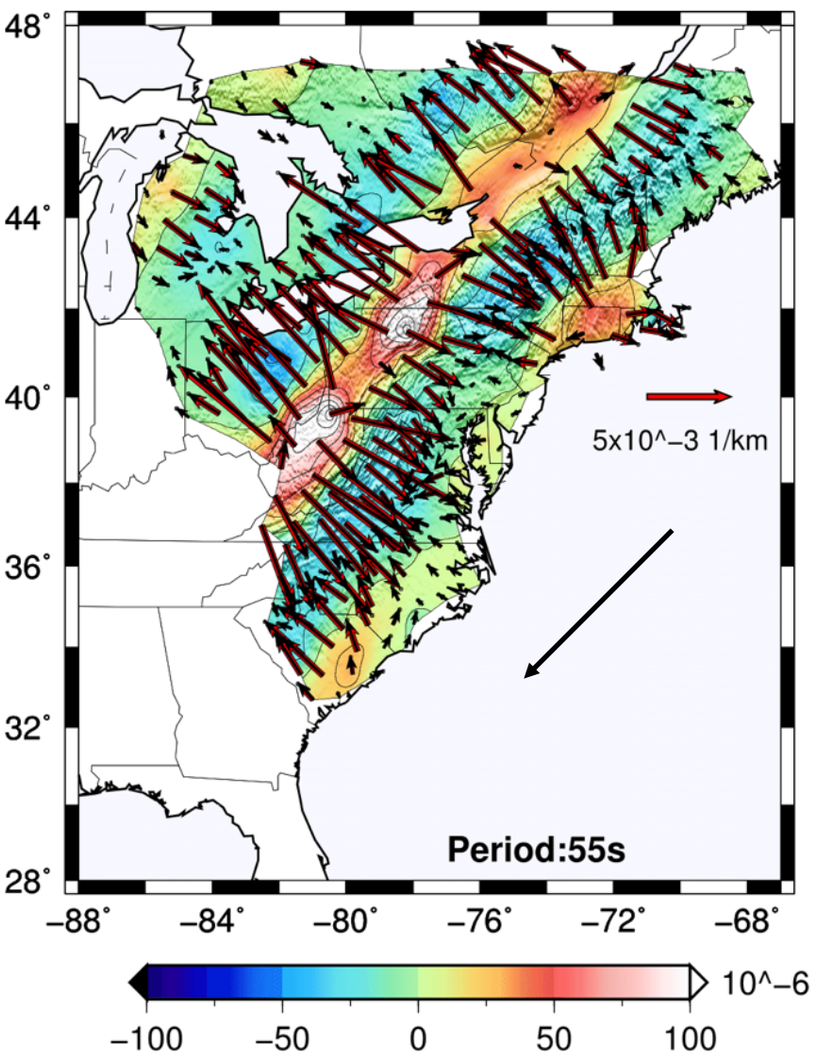

Gradient of A−coefficient

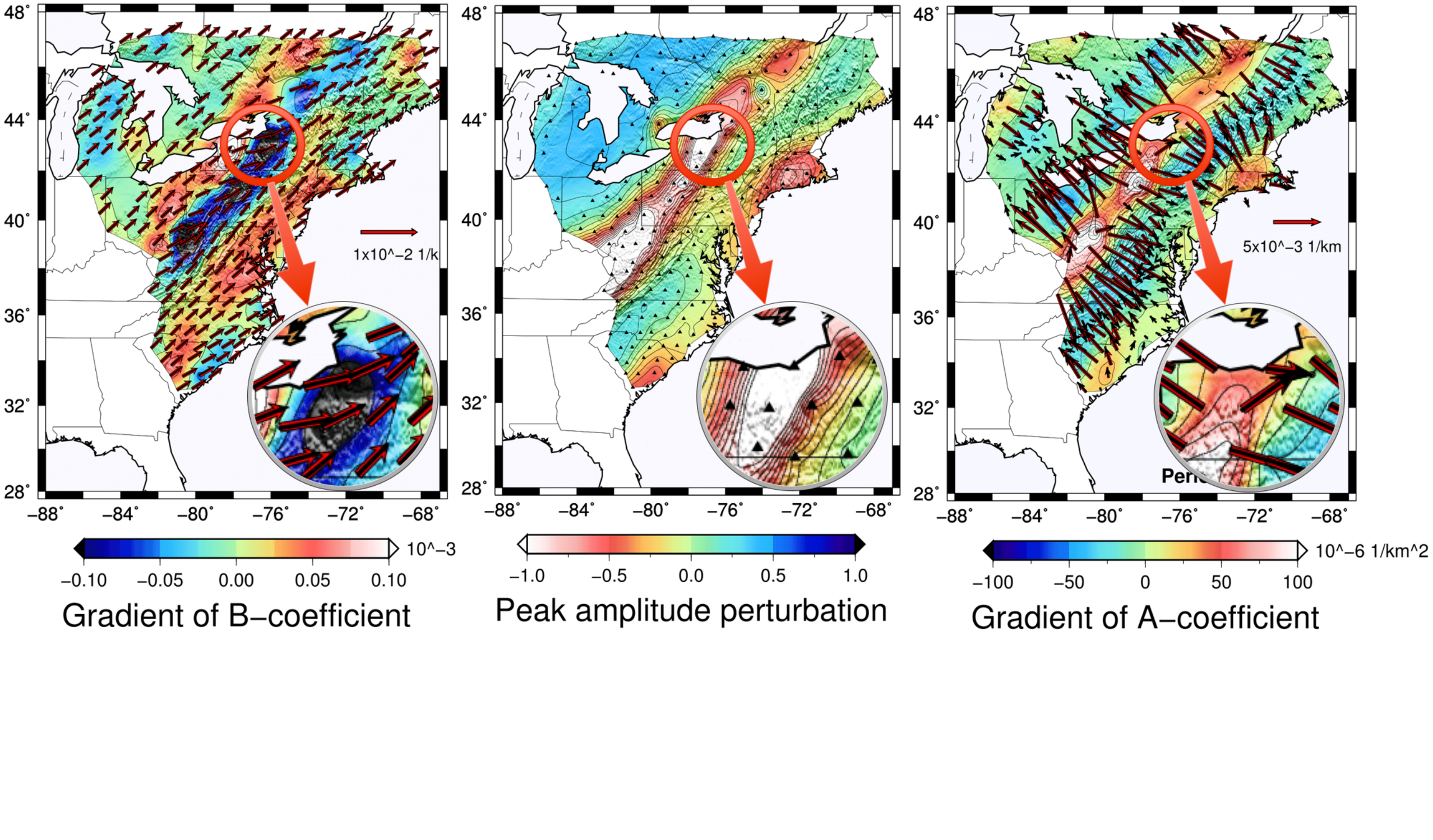
48˚
44˚
40˚
36˚
32˚
28˚
−88˚
−84˚
−80˚
−76˚
−72˚
−68˚
1x10^−2 1/k
10^−3
−0.10
−0.05
0.00
0.05
0.10
Gradient of B−coefficient
−1.0
−0.5
0.0
0.5
1.0
Peak amplitude perturbation
5x10^−3 1/km
10^−6 1/km^2
−100
−50
0
50
100
Gradient of A−coefficient

How can this information be used to better delineate source and propagation/structural influences?

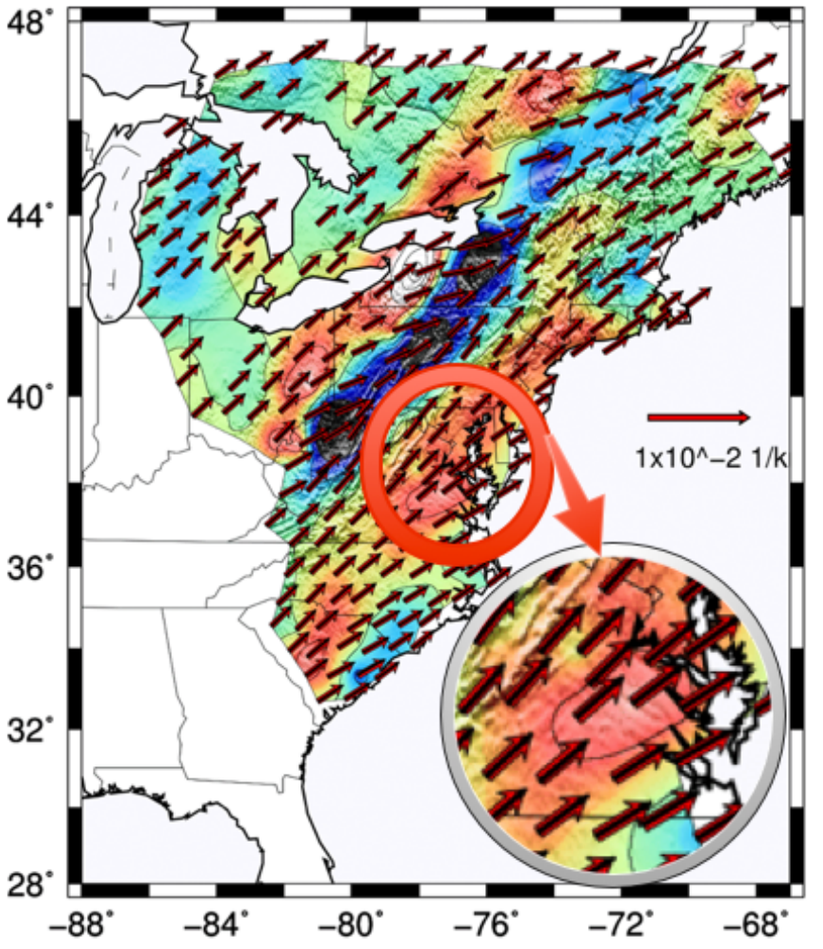

Gradient of B−coefficient

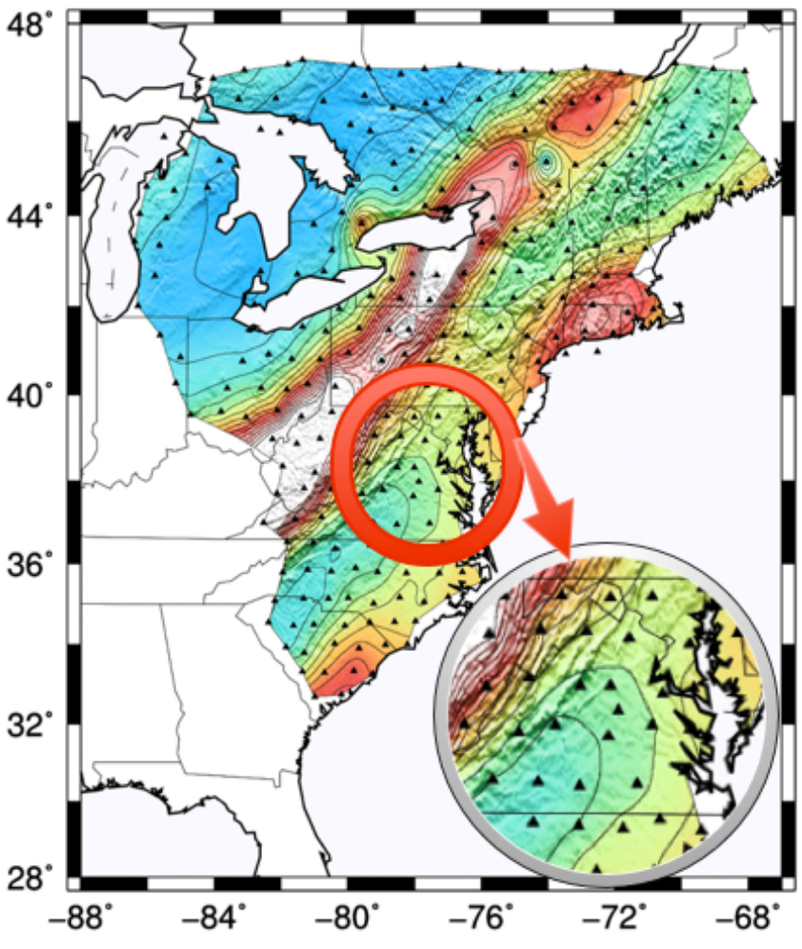

Peak amplitude perturbation

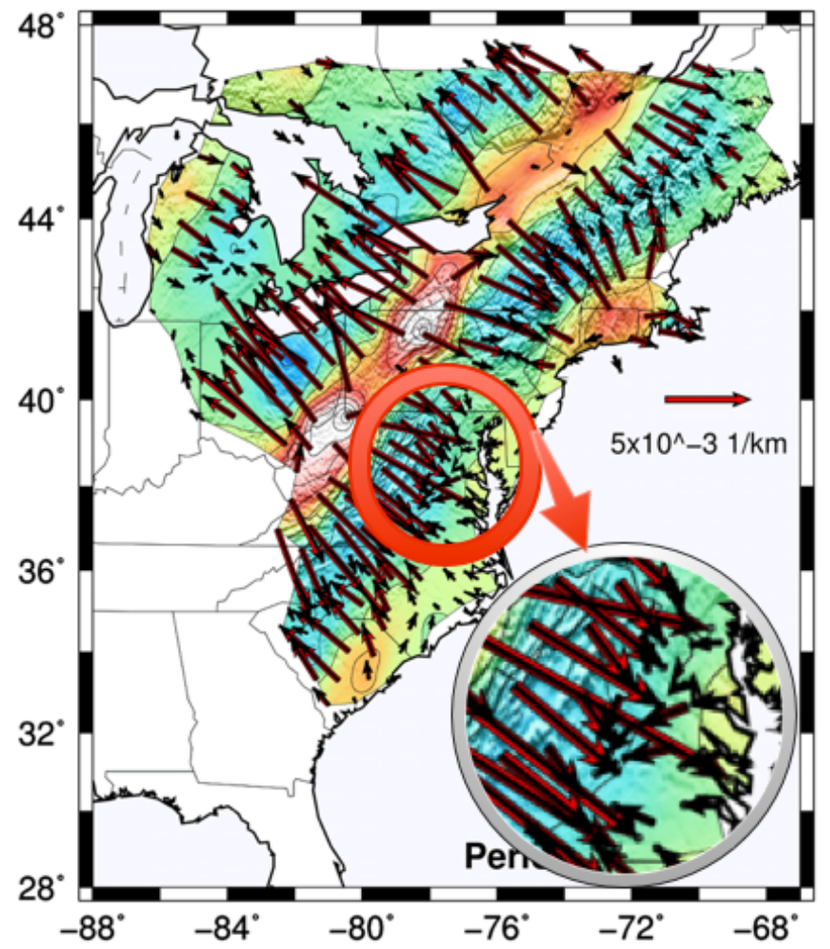

Gradient of A−coefficient

Outline

- Introduction and Motivation
- Wave Gradiometry and its Link with Helmholtz Equation Solution
- **Analysis of Six Events in Gulf of California**
- Analysis of Rayleigh Wave Isotropic Structural Phase velocity
- Inversion for Shear Velocity Models across the Continental U.S.
- Discussion and Conclusion

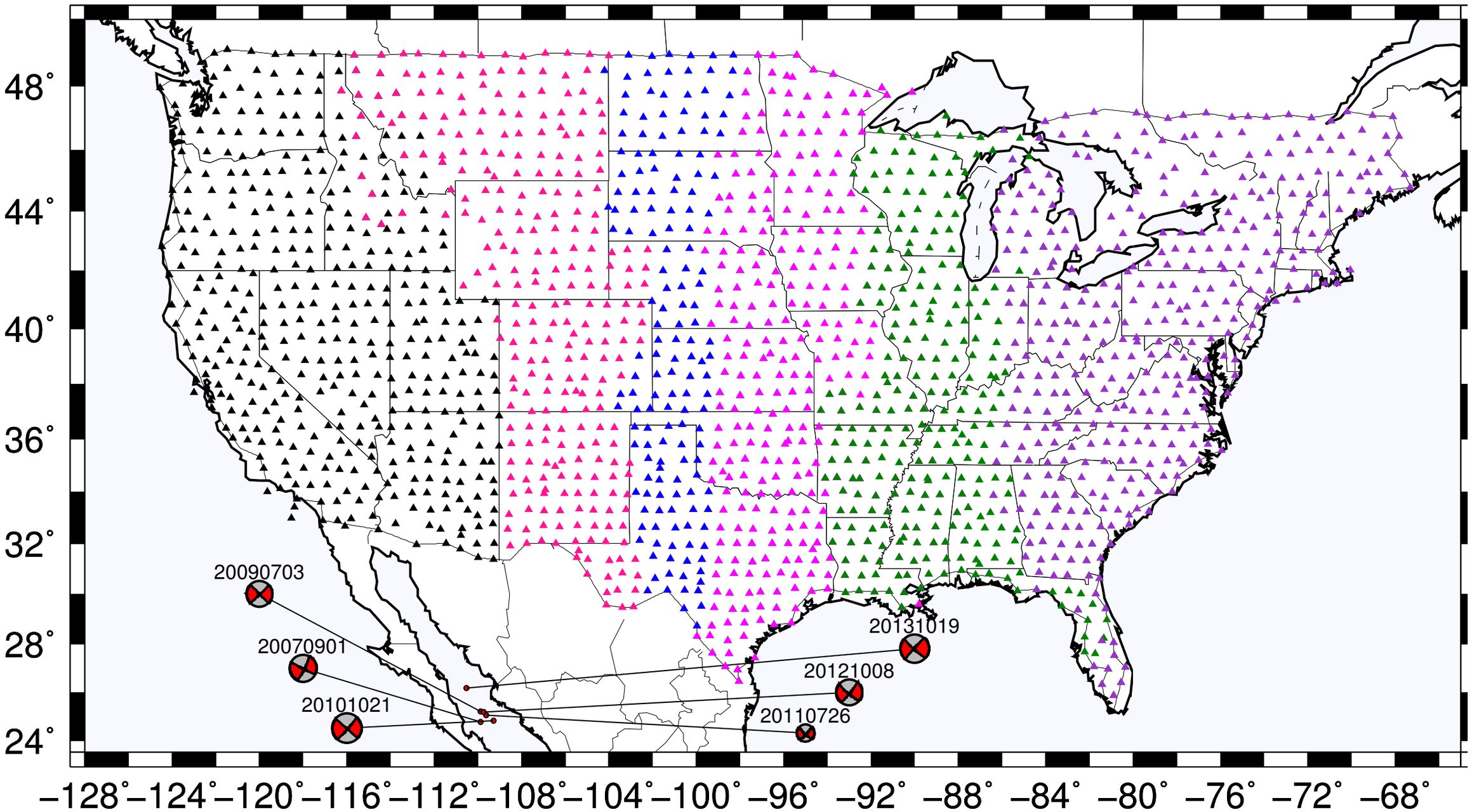

USArray TA station distribution map and the locations for six Gulf of California Earthquakes.

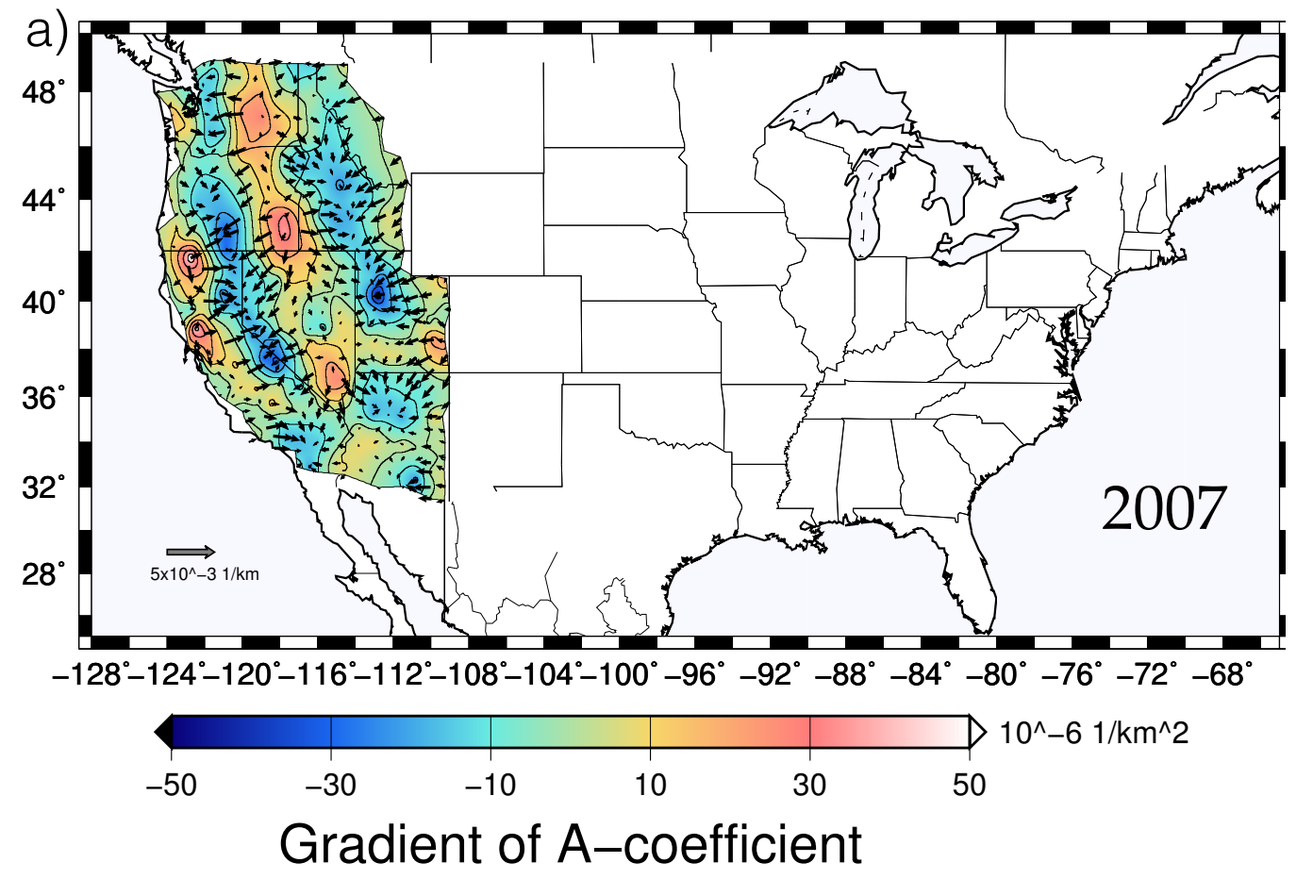

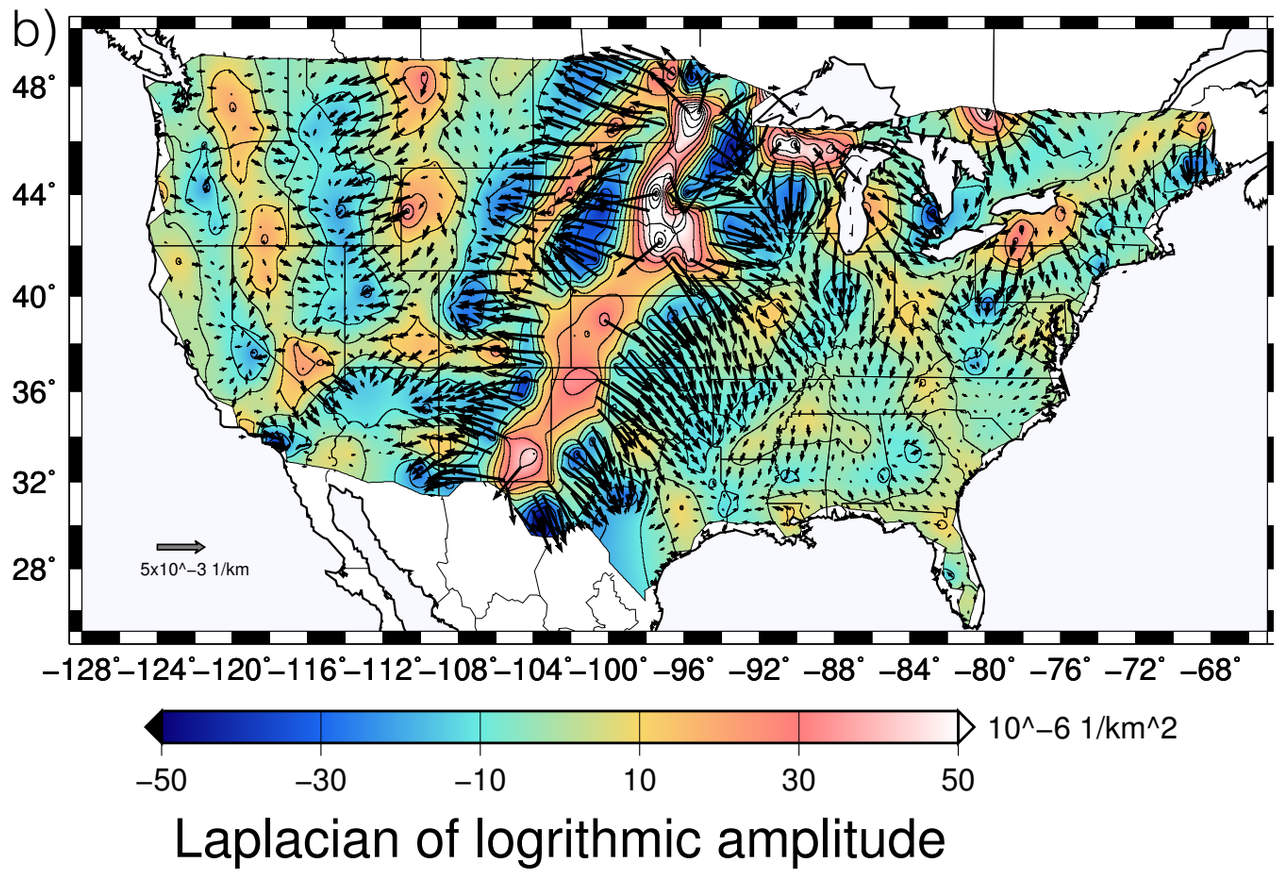

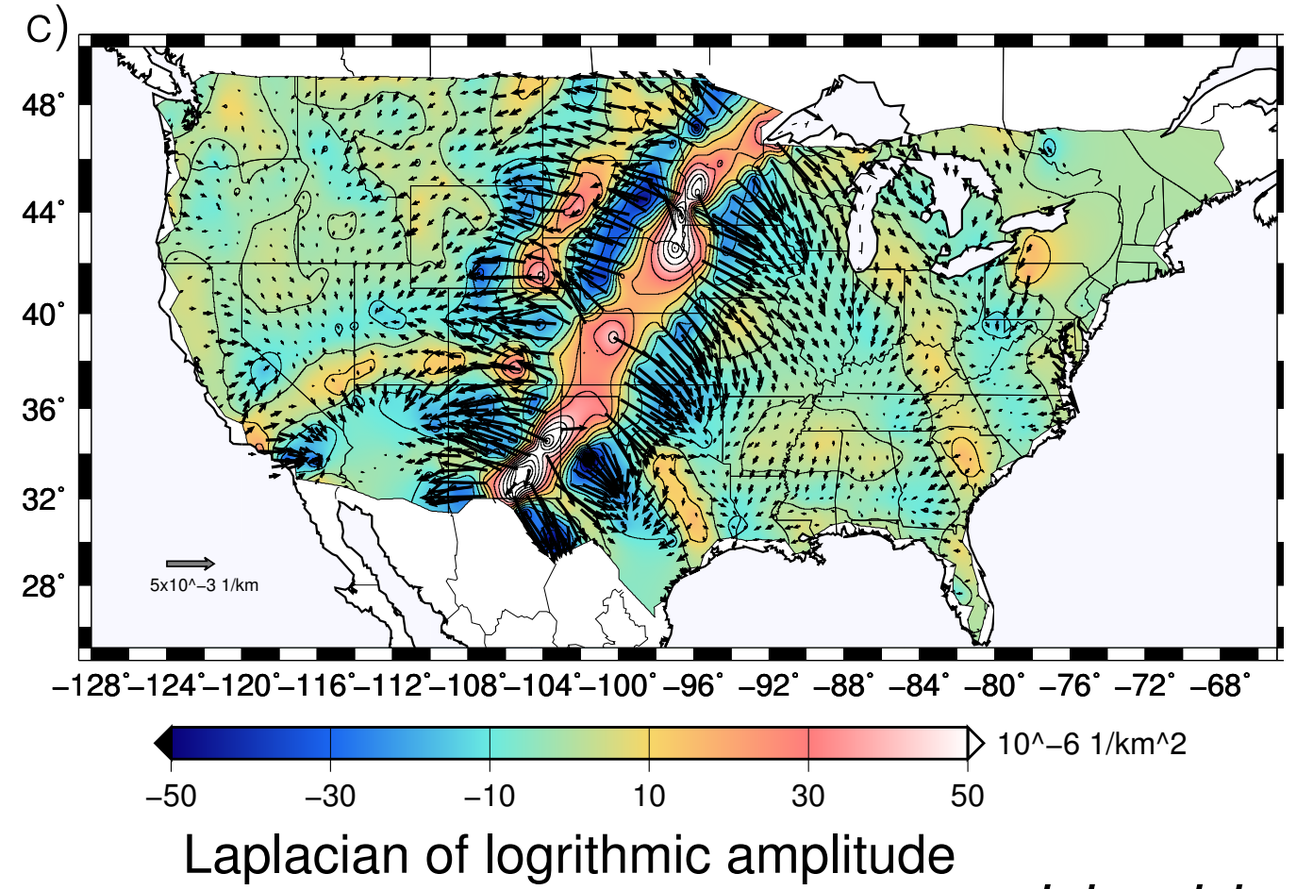

The 60 s Rayleigh wave gradiometry parameters: A-coefficient vectors and gradients for 2007 event obtained from (a) real records (b) synthetics computed by Hejun Zhu at UT Dallas and (c) Global ShakeMovie.

Liu, Holt, and Zhu, 2016, JGR, In revision

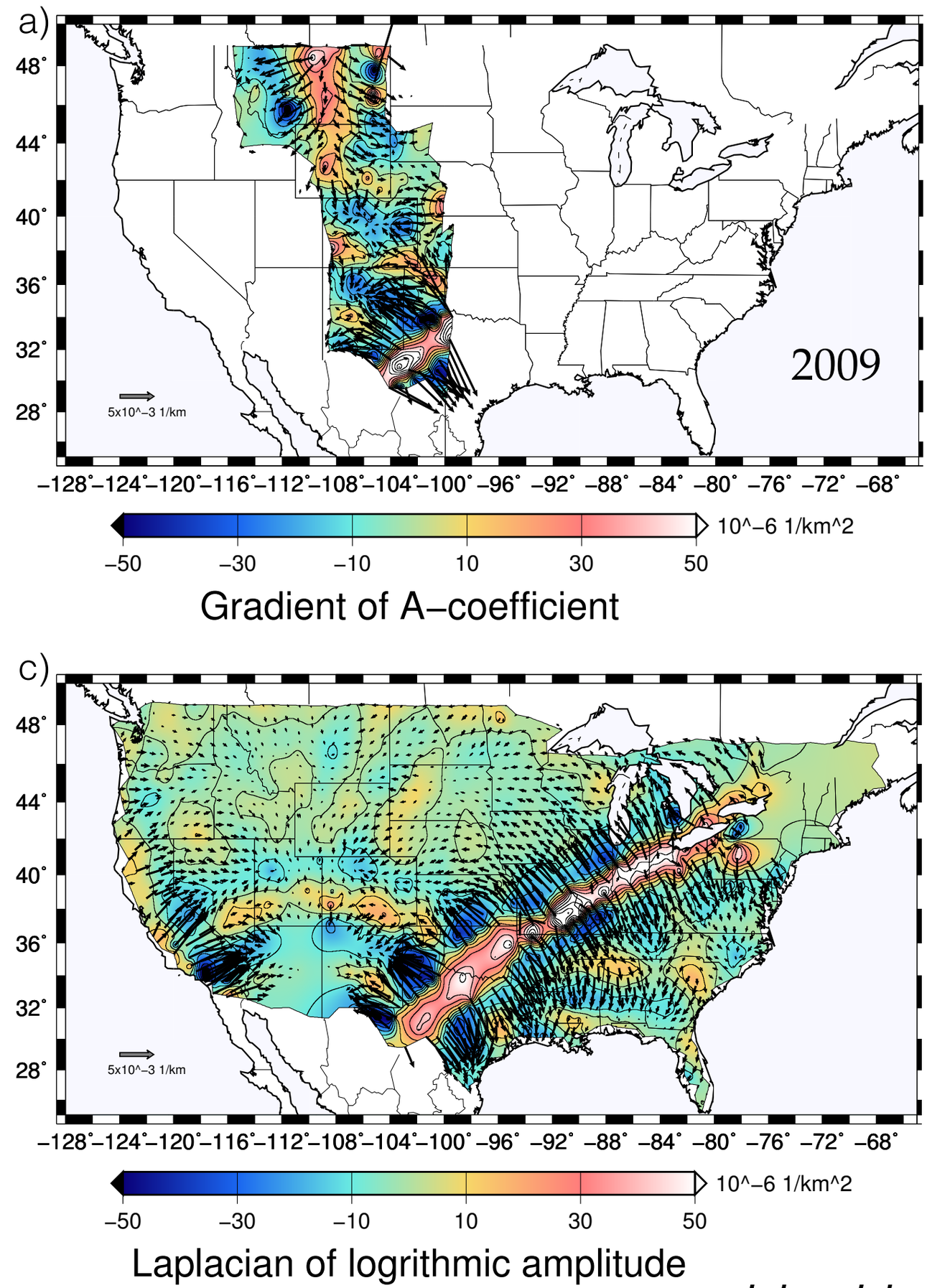

The 60 s Rayleigh wave gradiometry parameters: A-coefficient vectors and gradients for 2009 event obtained from (a) real records (b) synthetics provided by Hejun Zhu at UT Dallas and (c) Global ShakeMovie.

Liu, Holt, and Zhu, 2016, JGR, In revision

a)

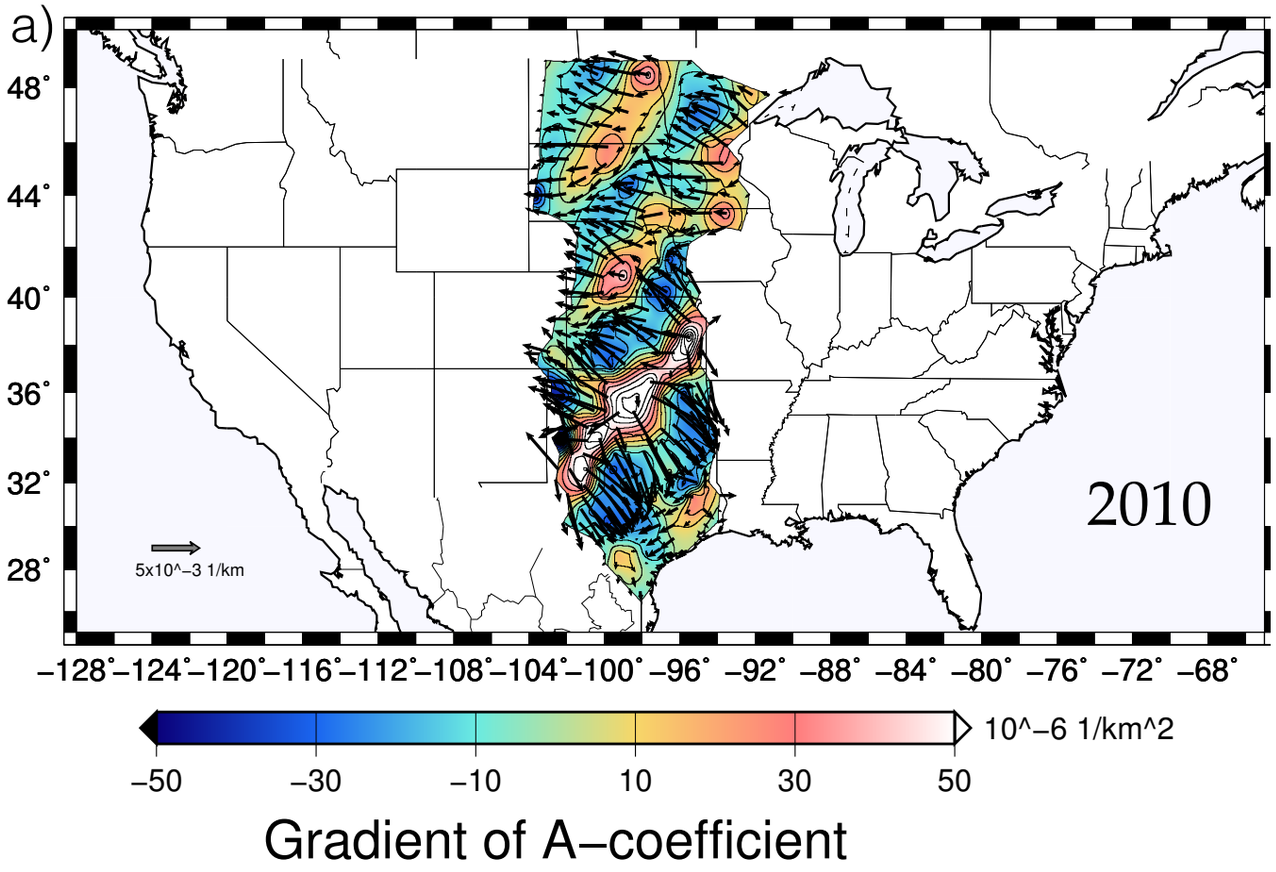
48˚
44˚
40˚
36˚
32˚
28˚
5x10^−3 1/km
2010
−128˚ −124˚ −120˚ −116˚ −112˚ −108˚ −104˚ −100˚ −96˚ −92˚ −88˚ −84˚ −80˚ −76˚ −72˚ −68˚
10^−6 1/km^2
−50 −30 −10 10 30 50
Gradient of A−coefficient

b)

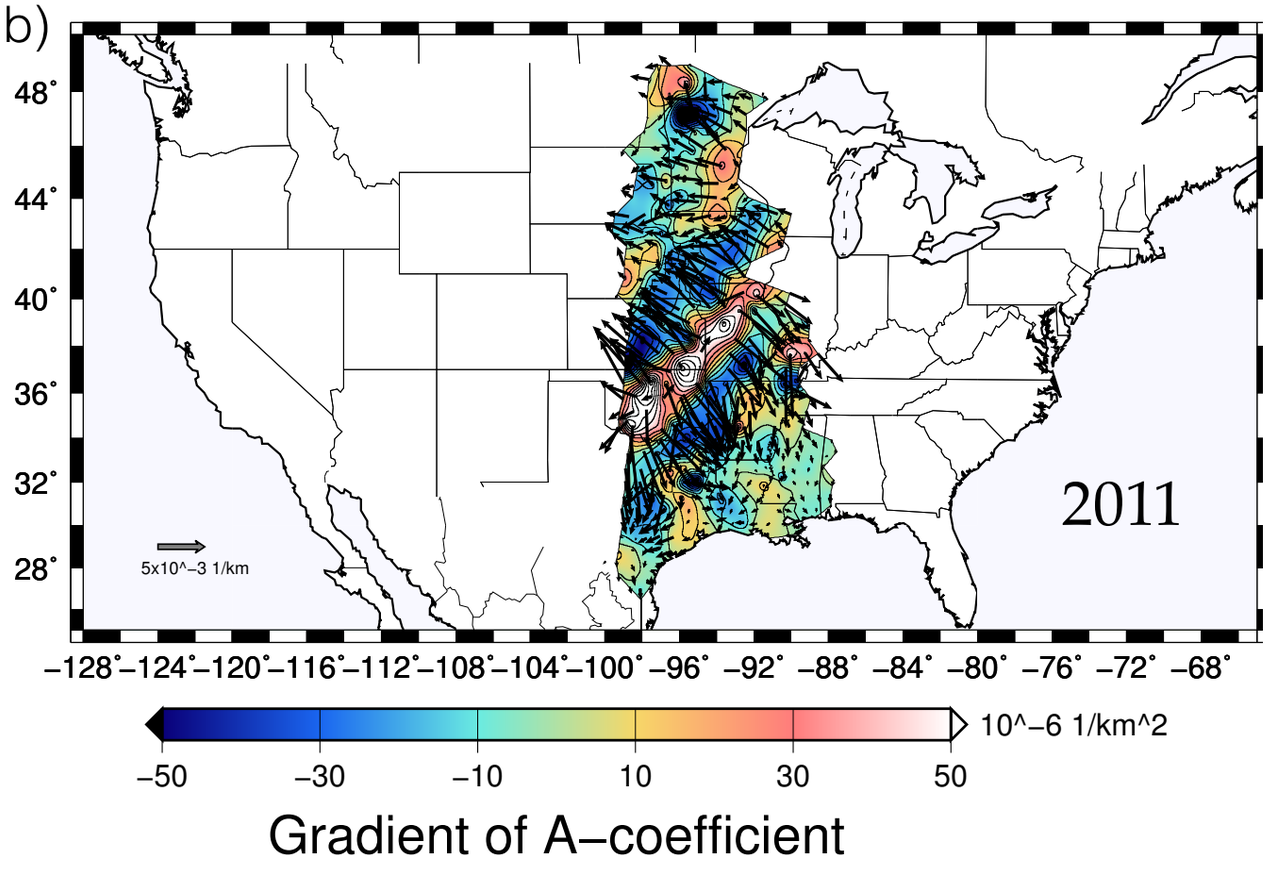
48˚
44˚
40˚
36˚
32˚
28˚
5x10^−3 1/km
2011
−128˚ −124˚ −120˚ −116˚ −112˚ −108˚ −104˚ −100˚ −96˚ −92˚ −88˚ −84˚ −80˚ −76˚ −72˚ −68˚
10^−6 1/km^2
−50 −30 −10 10 30 50
Gradient of A−coefficient

c)

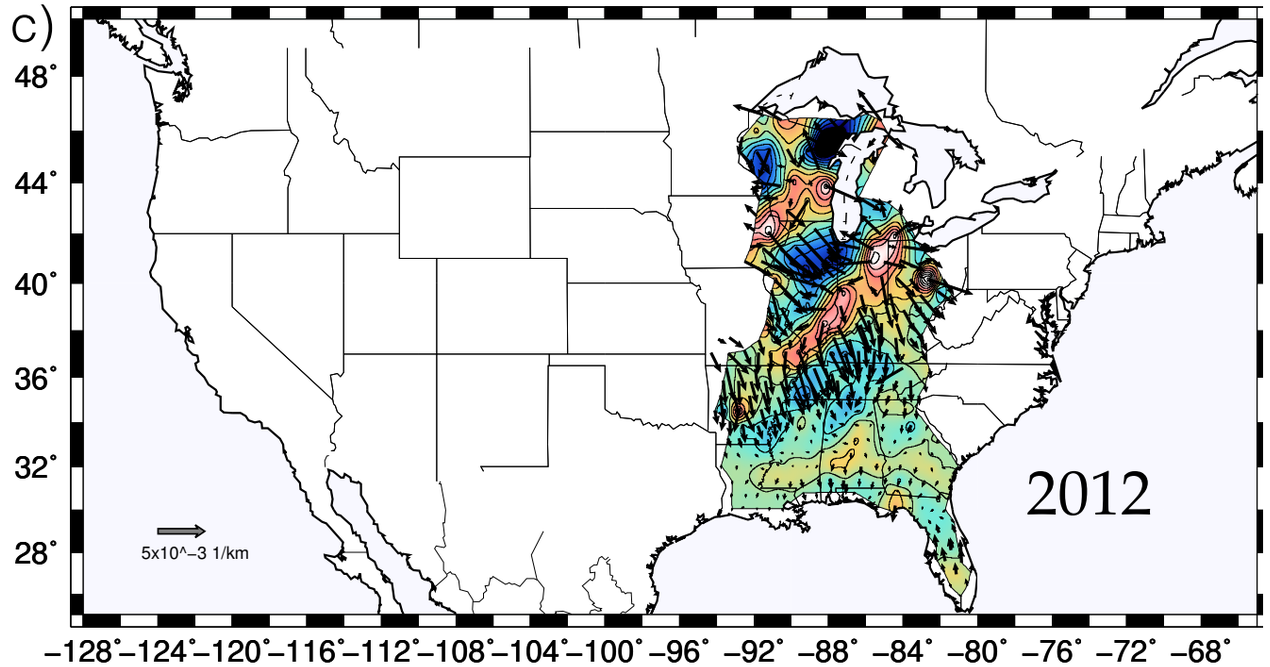
48˚
44˚
40˚
36˚
32˚
28˚
5x10^−3 1/km
2012
−128˚ −124˚ −120˚ −116˚ −112˚ −108˚ −104˚ −100˚ −96˚ −92˚ −88˚ −84˚ −80˚ −76˚ −72˚ −68˚
10^−6 1/km^2
−50 −30 −10 10 30 50
Gradient of A−coefficient

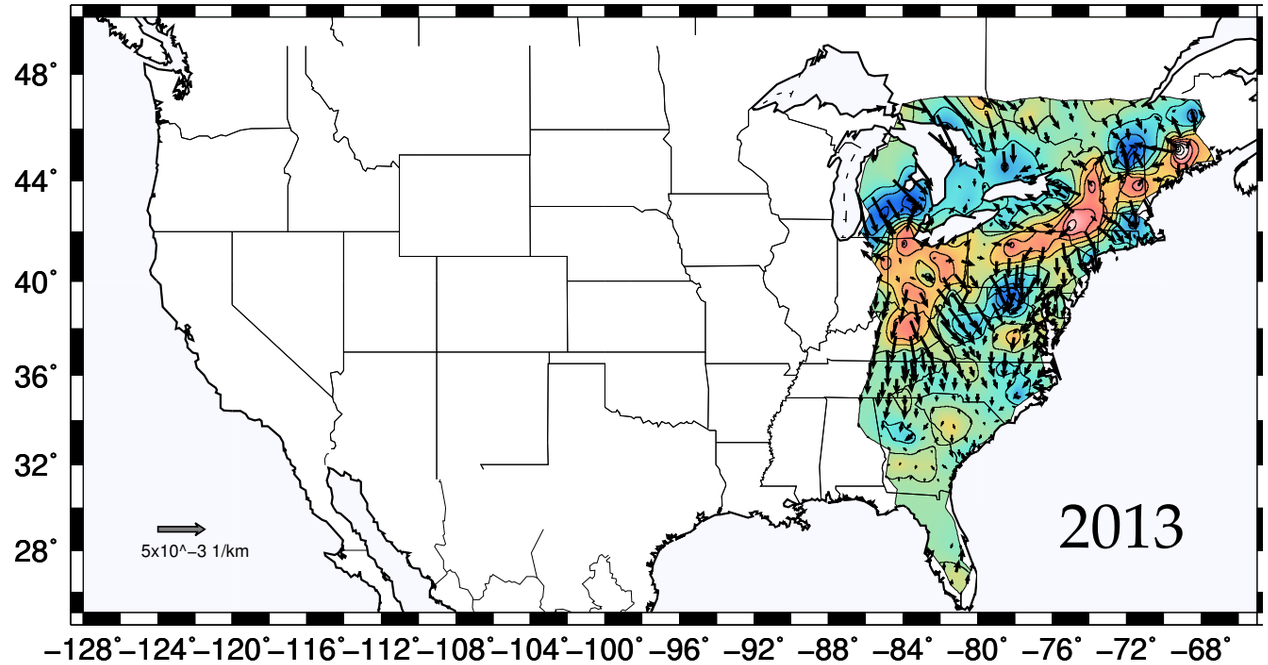
48˚
44˚
40˚
36˚
32˚
28˚
5x10^−3 1/km
2013
−128˚ −124˚ −120˚ −116˚ −112˚ −108˚ −104˚ −100˚ −96˚ −92˚ −88˚ −84˚ −80˚ −76˚ −72˚ −68˚
10^−6 1/km^2
−50 −30 −10 10 30 50
Gradient of A−coefficient

a)

b)

c)

d)

Predicted

Predicted

5x10^−3 1/km

10^−1s/km

10^−6 1/km^2

10^−3 1/km^2

−50 −30

−1.0 −0.8 −0.6 −0.4

50

1.0

48° 44° 40° 36° 32° 28°

−128° −124° −120° −116° −112°

−80° −76° −72° −68°

a)

Observed

b)

Predicted

48° 44° 40° 36° 32° 28°

−128° −124° −120° −116° −112° −108° −104° −100° −96° −92° −88° −84° −80° −76° −72° −68°

−15 −13 −11 −9 −7 −5 −3 −1 1 3 5 7 9 11 13 15 1/deg

Radiation pattern

c)

Observed

d)

Predicted

48° 44° 40° 36° 32° 28°

−128° −124° −120° −116° −112° −108° −104° −100° −96° −92° −88° −84° −80° −76° −72° −68°

−3 −2 −1 0 1 2 3 1/1000km

−3.0 −2.5 −2.0 −1.5 −1.0 −0.5 0.0 0.5 1.0 1.5 2.0 2.5 3.0 1/1000km

Geometrical spreading

Liu, Holt, and Zhu, 2016, JGR, In revision

Outline

- Introduction and Motivation
- Wave Gradiometry and its Link with Helmholtz Equation Solution
- Analysis of Six Events in Gulf of California
- **Analysis of Rayleigh Wave Isotropic Structural Phase velocity**
- Inversion for Shear Velocity Models across the Continental U.S.
- Discussion and Conclusion

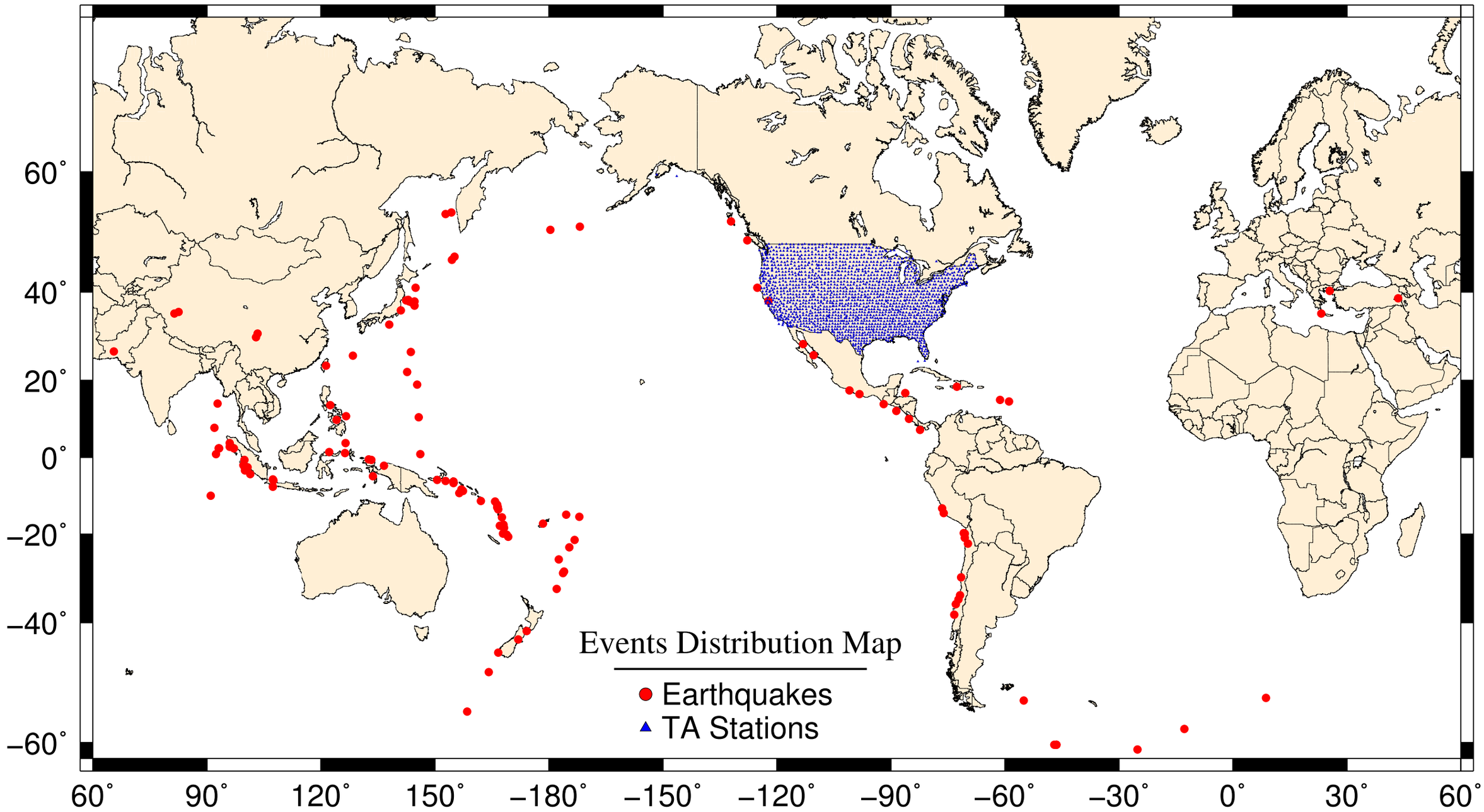

Wave gradiometry is applied to 700 earthquakes between 2007 and 2014, with magnitudes greater than 5.0 and focal depths shallower than 50 km recorded by 1,739 TA stations.

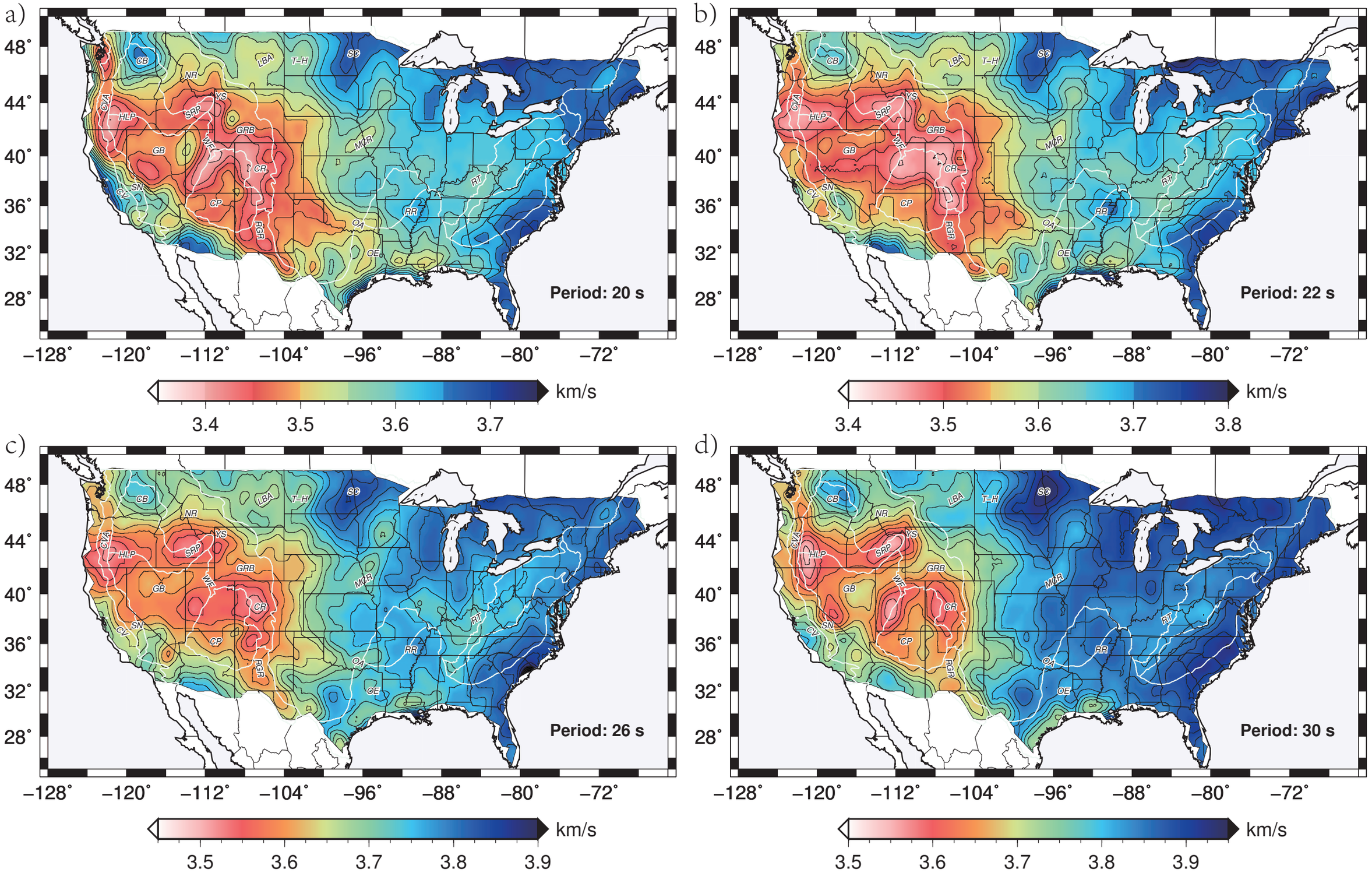

The 20 - 30 s Rayleigh wave Isotropic phase velocity

Liu and Holt, 2016, G-Cubed, In Review

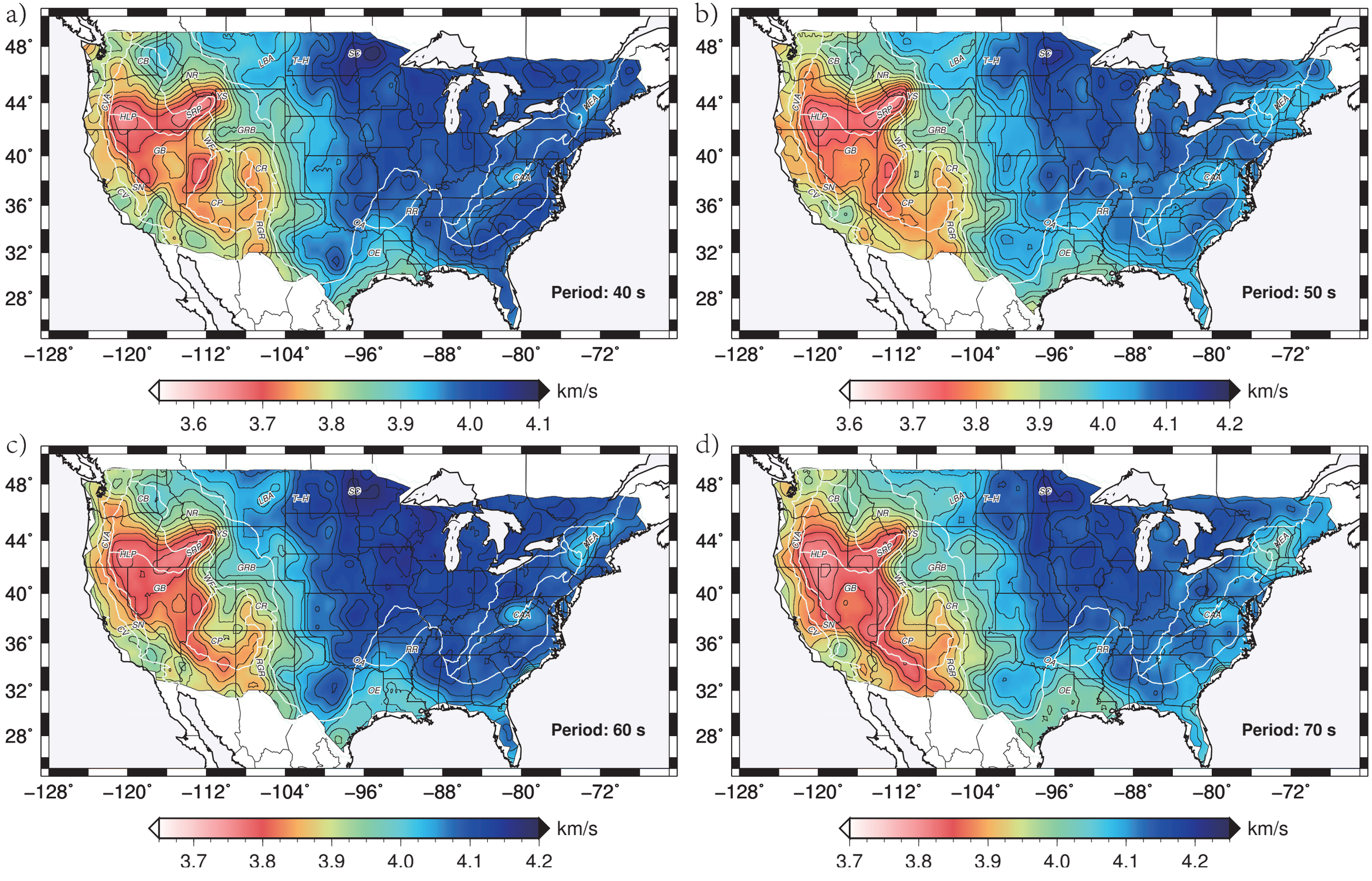

The 40 - 70 s Rayleigh wave Isotropic phase velocity

Liu and Holt, 2016, G-Cubed, In Review

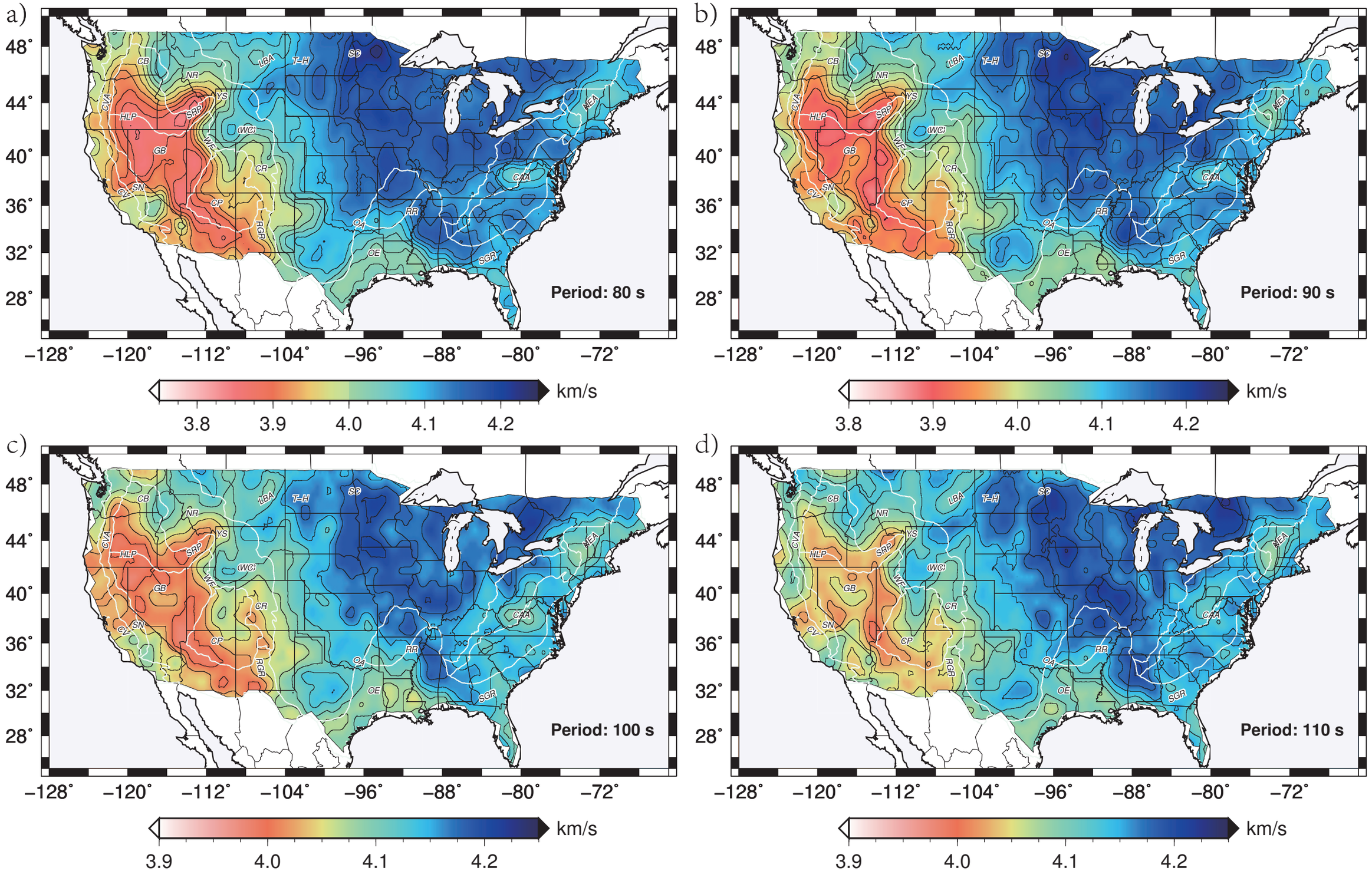

The 80 - 110 s Rayleigh wave Isotropic phase velocity

Liu and Holt, 2016, G-Cubed, In Review

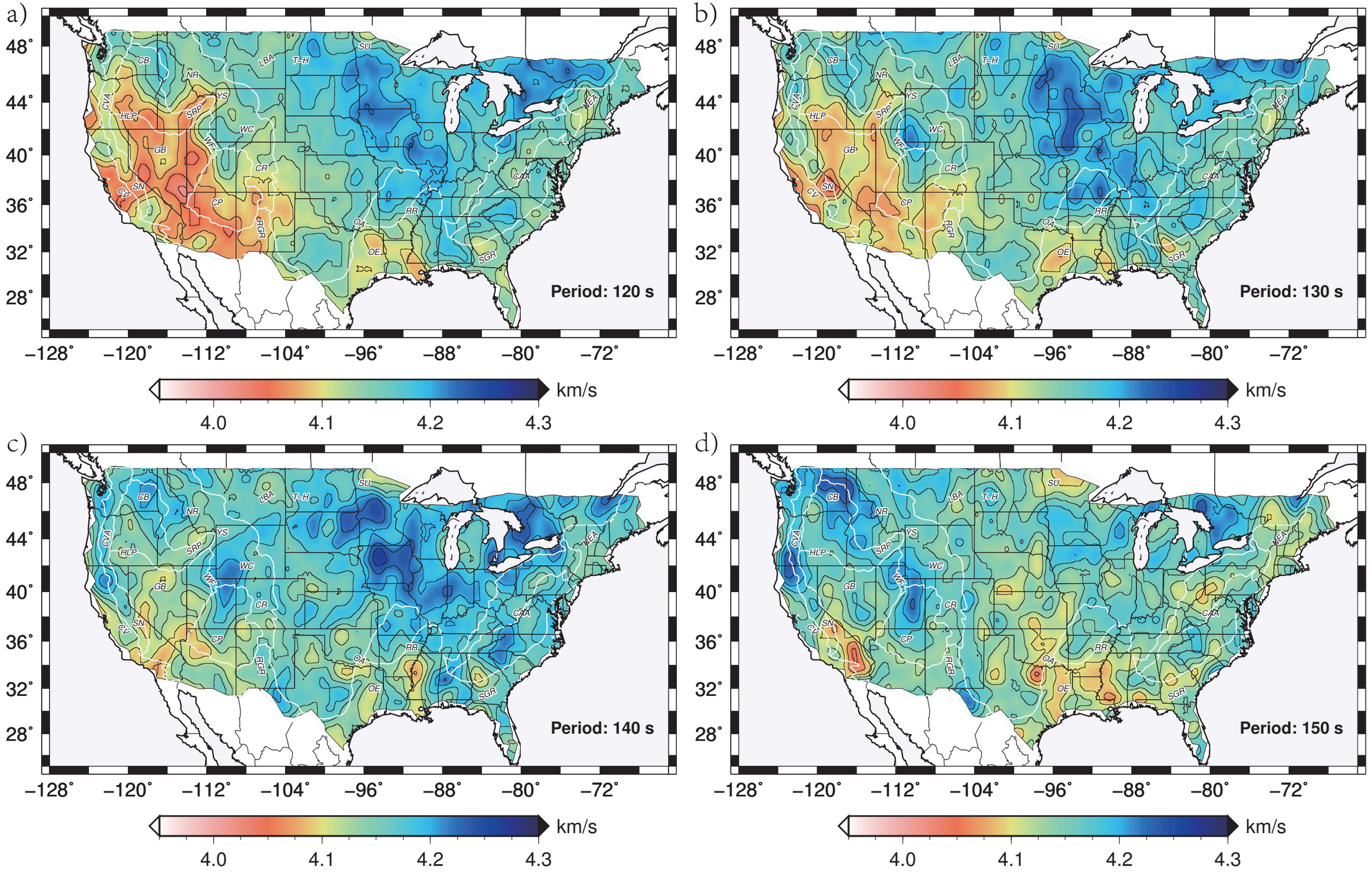

The 120 - 150 s Rayleigh wave Isotropic phase velocity

Liu and Holt, 2016, G-Cubed, In Review

Standard errors for dynamic versus structural phase velocity

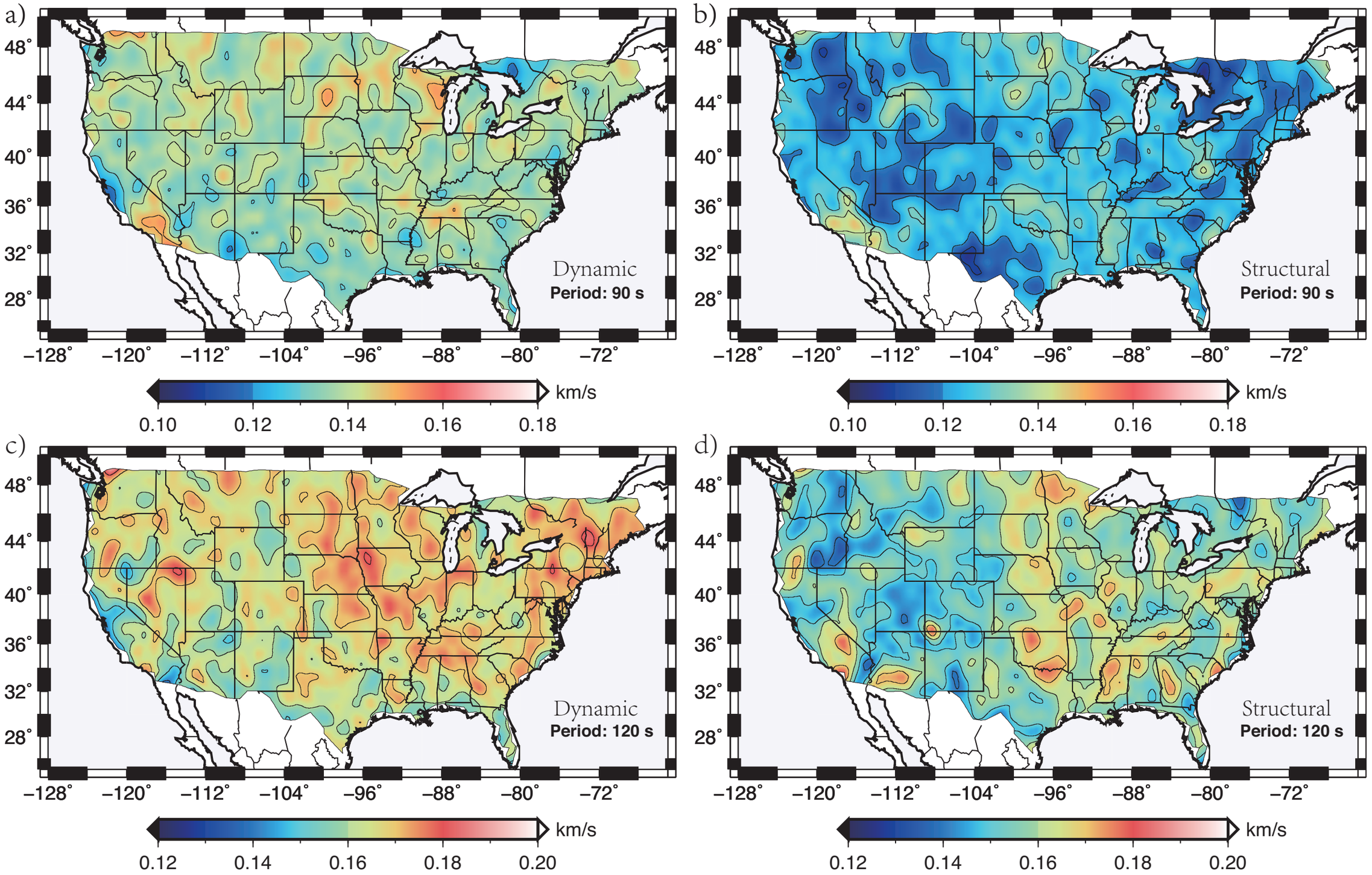

The standard deviations for 90 s and 120 s Rayleigh wave (a,c) dynamic and (c,d) structural phase velocities.

Outline

- Introduction and Motivation
- Wave Gradiometry and its Link with Helmholtz Equation Solution
- Analysis of Six Events in Gulf of California
- Analysis of Rayleigh Wave Isotropic Structural Phase velocity
- **Inversion for Shear Velocity Models across the Continental U.S.**
- Discussion and Conclusion

Joint inversion of phase velocities for shear velocity structure from ambient noise and wave gradiometry [*Porter, Liu, Holt*, 2016, GRL]

1) Ambient noise tomo. for 8s < T < 40s

2) Gradiometry for 20s < T < 150 s

3) Results were averaged for 20-40s

4) Iterative least-squares inversion using method of Herrmann and Ammon [2002]

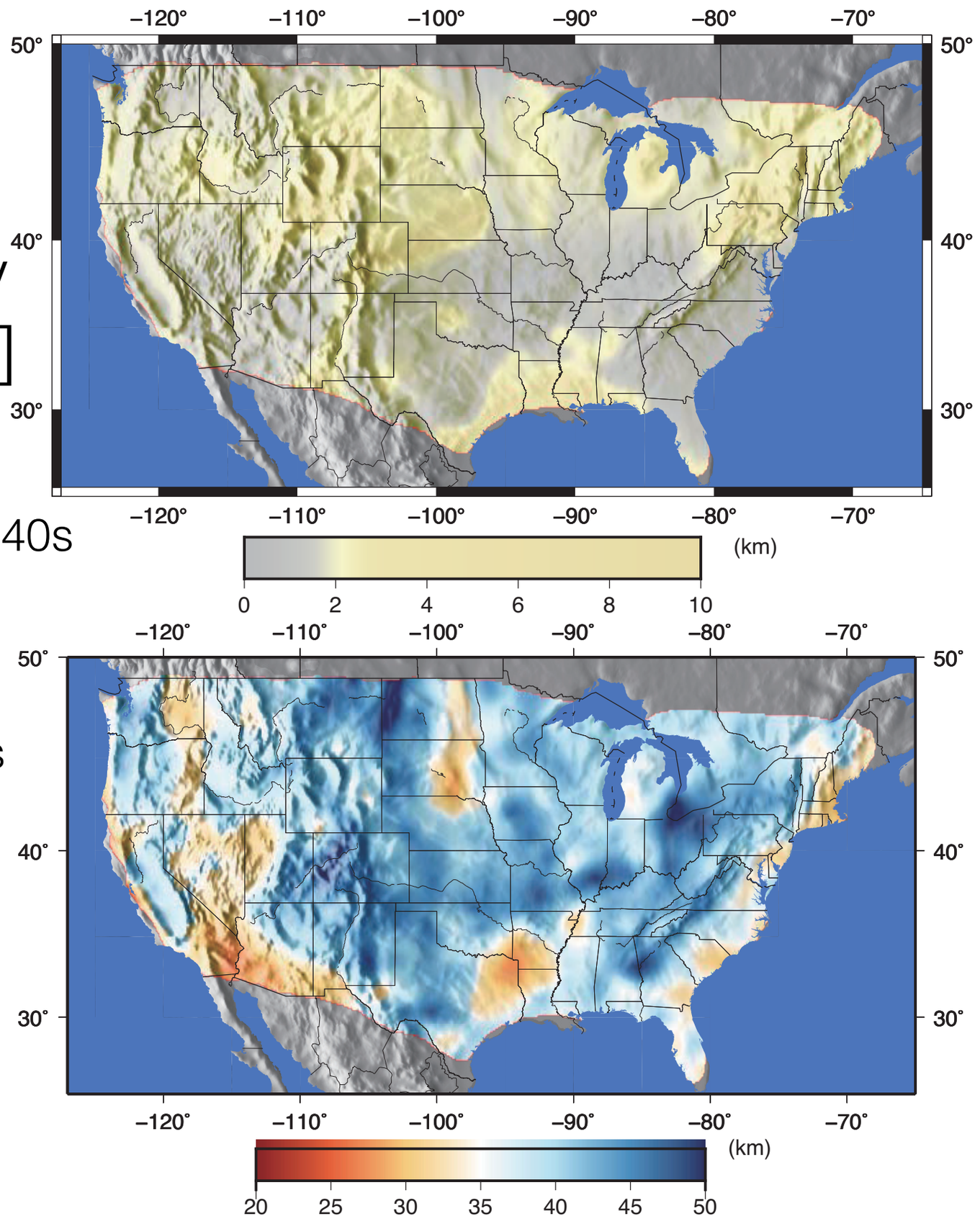

Map view of the (a) crustal and (b) sediment thickness model used in *Porter et al*. [2016].

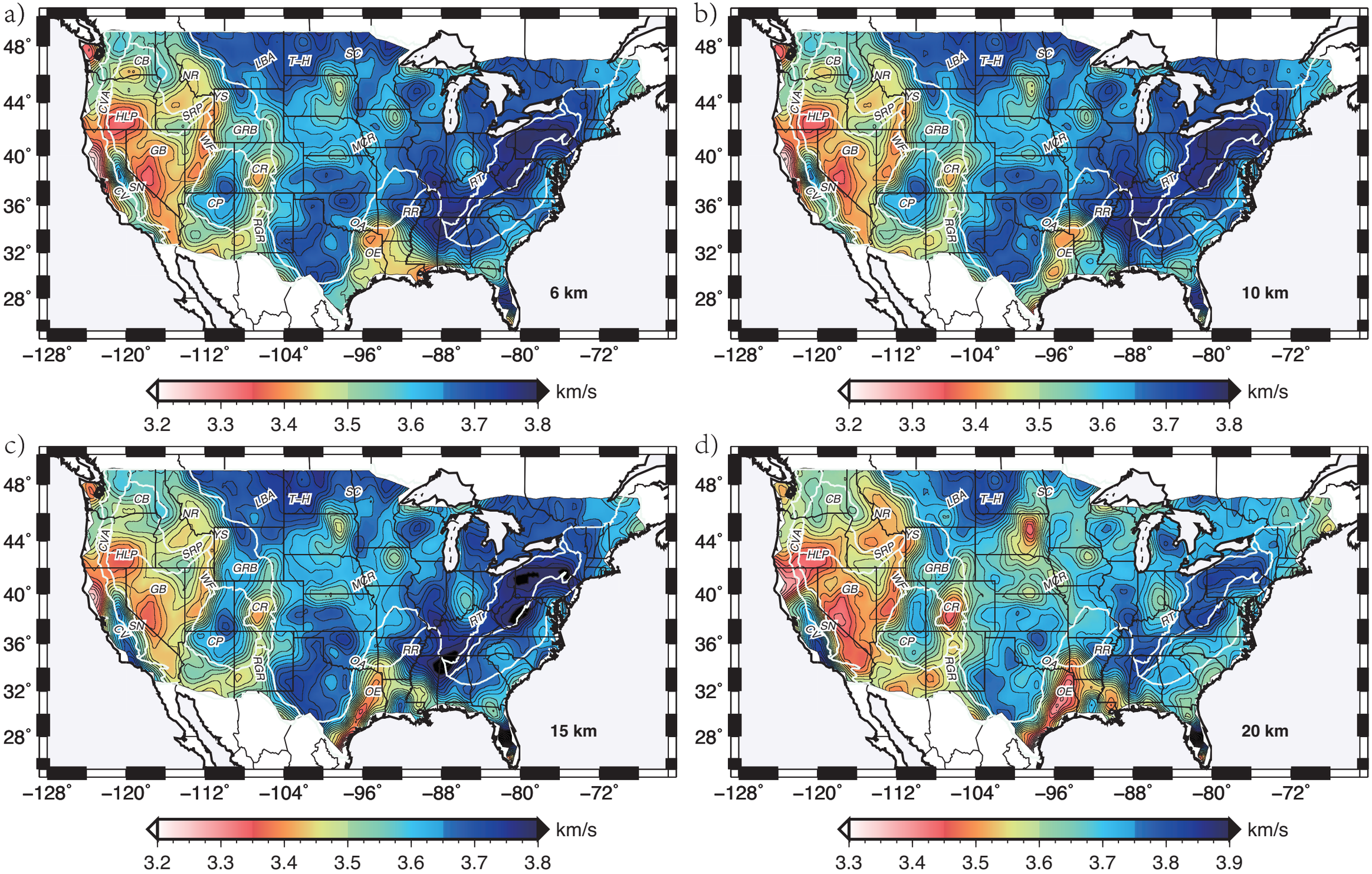

The shear velocity within depth range of 6 - 20 km

Porter, Liu and Holt, 2016, GRL

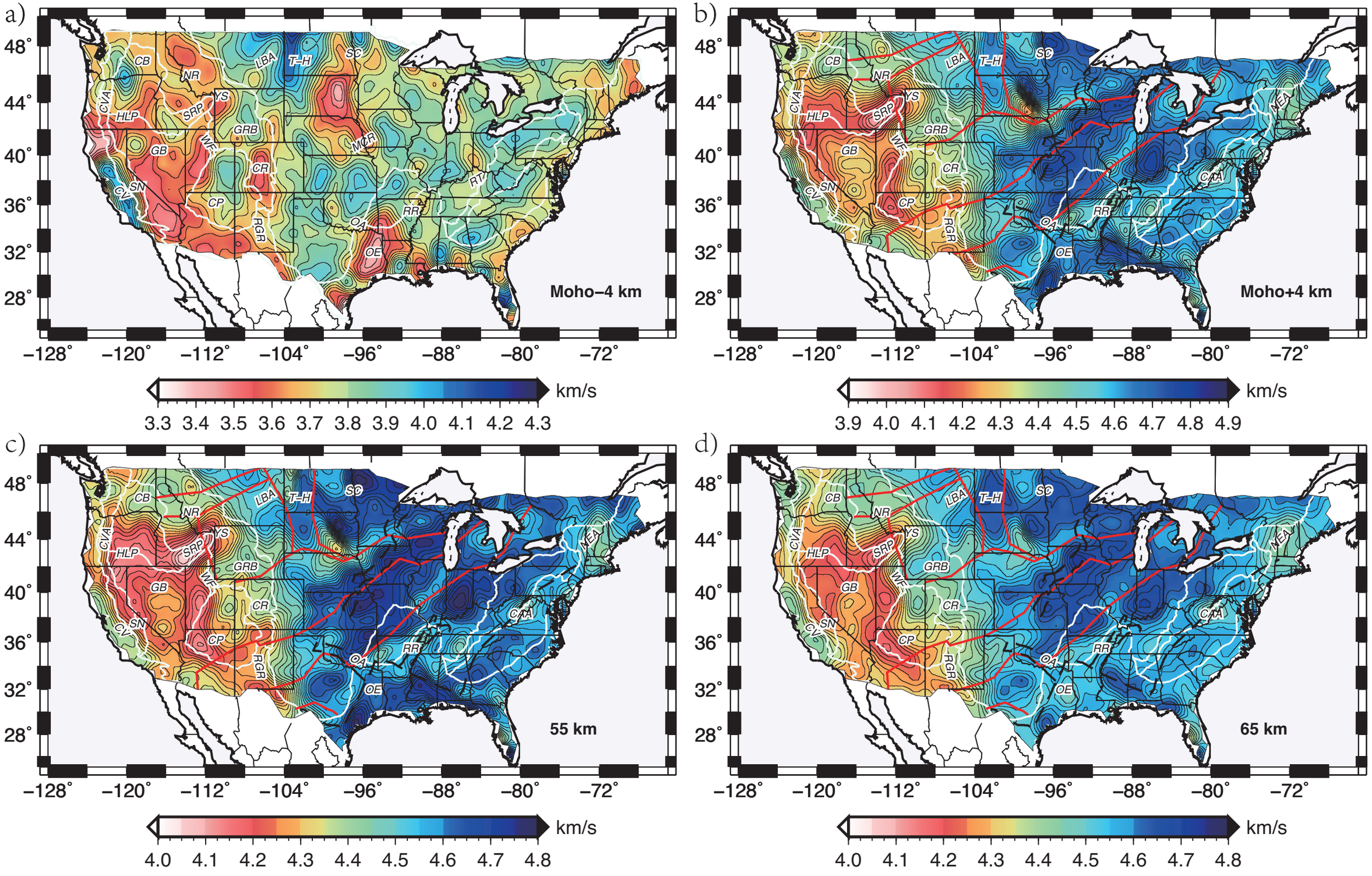

The shear velocity within depth range of Moho-4 - 65 km. Red lines show approximate tectonic province boundaries following Whitmeyer and Karlstrom [2007] and black dashed lines show rift and collisional boundaries.

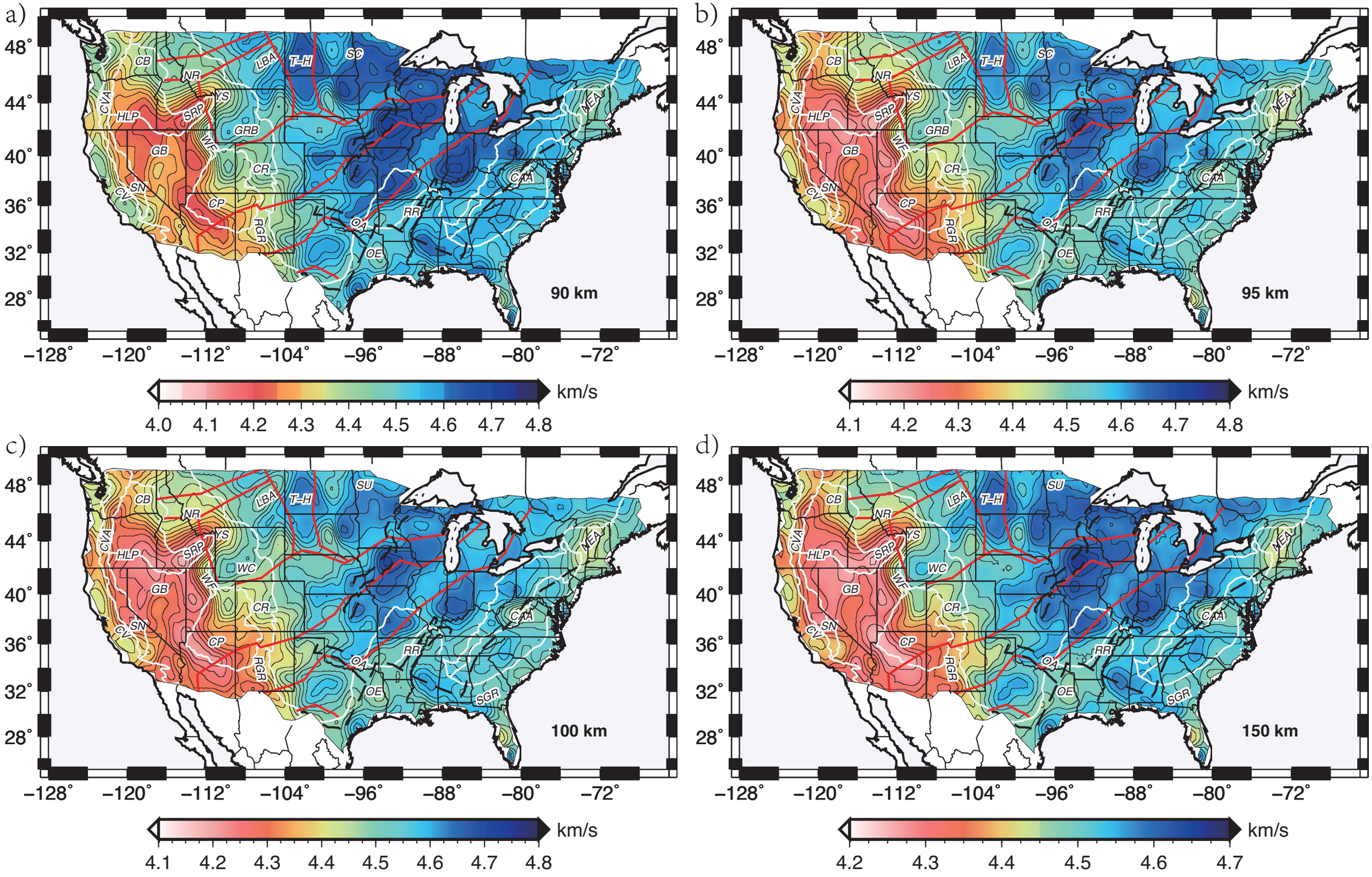

The shear velocity within depth range of 90 - 150 km

Porter, Liu and Holt, 2016, GRL

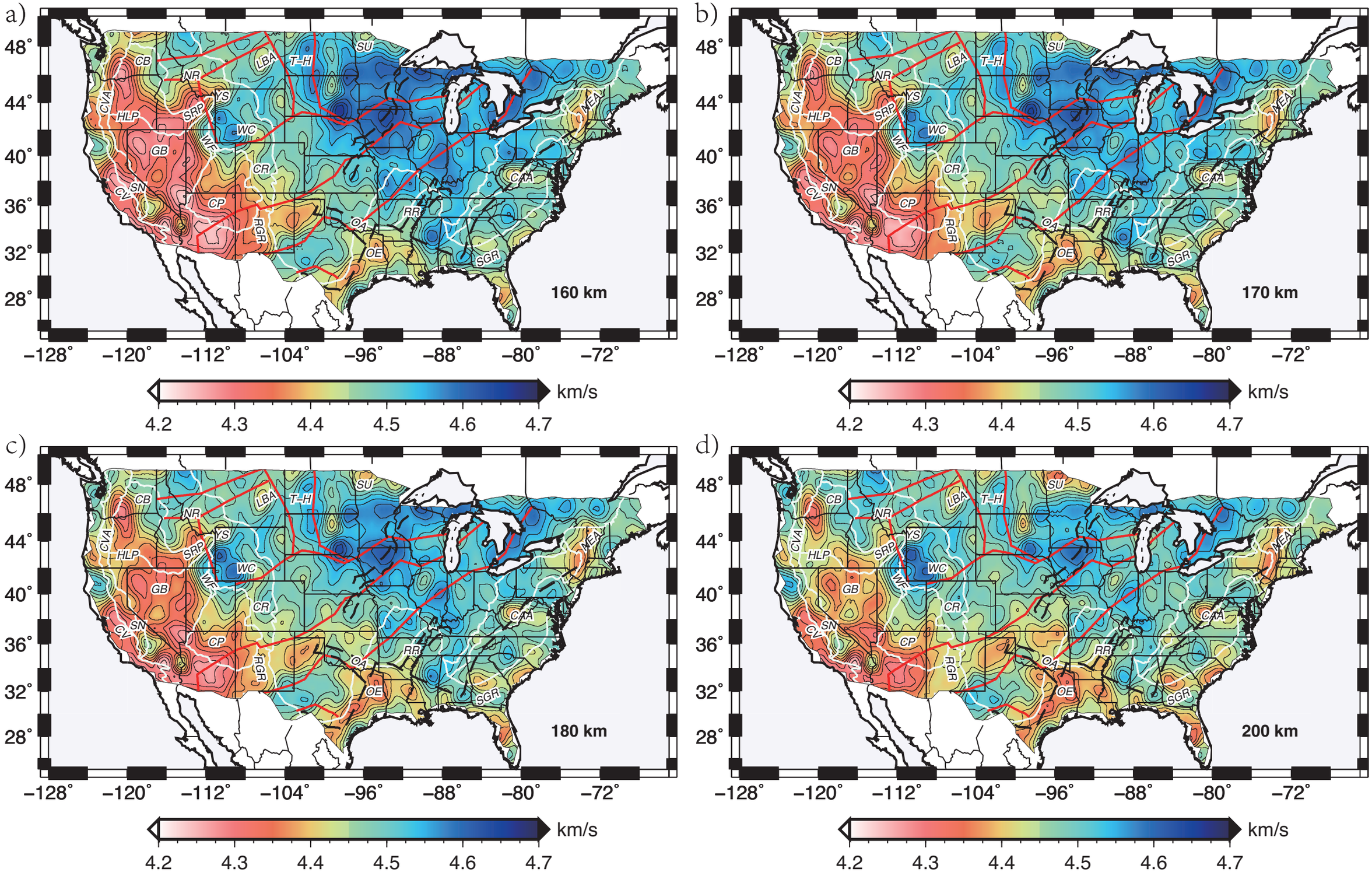

The shear velocity within depth range of 160 - 200 km

Porter, Liu and Holt, 2016, GRL

Conclusions

1) Wave gradiometry uses both amplitude and travel time information to infer dynamic phase velocity, back azimuth, radiation pattern and geometrical spreading. Gradiometry parameters are combined with dynamic phase velocity to generate structural phase velocity, which depends on the properties of the medium only.

2) Analysis of the wavefields from six events that occurred in the Gulf of California shows remarkable features of the wavefield that link the focusing and defocusing of energy with significant amplitude variations. The comparison between results from two sets of synthetic calculations and real records show that gradiometry parameters are sensitive to input structure.

3) The isotropic phase velocity maps across the contiguous U.S show interesting variations that correlate with major geological provinces and show the depth extent of both crust and upper mantle velocity anomalies.

4) The broad depth range (8 km - 200 km) of the shear models allow us to examine the lithospheric structure of the continent in great detail and associate modern subsurface features in the crust and upper mantle to the formation of the continent and orogenic events that impacted the structure and evolution of the lithosphere in North America.

Thank you!

Questions?

Displacement gradients are determined using interpolation method of Haines and Holt [1993] and Beavan and Haines [2001]

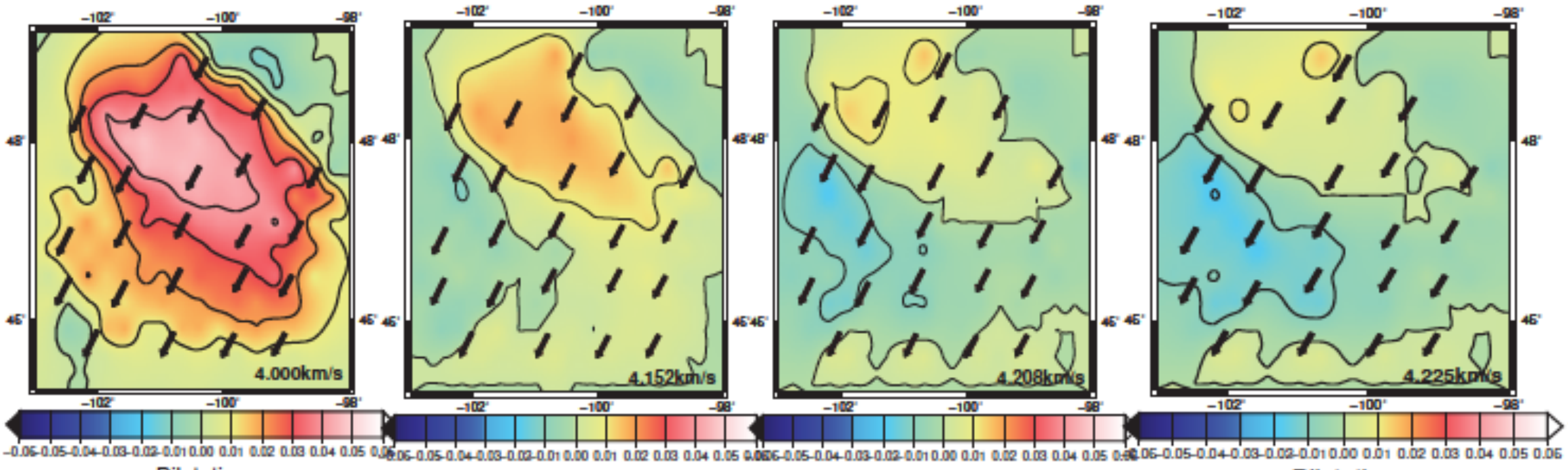

$$\mathbf{u}(\hat{\mathbf{r}}) = r\mathbf{W}(\hat{\mathbf{r}}) \times \hat{\mathbf{r}}$$

$$\varepsilon_{\phi\phi} = \frac{1}{\cos\theta}\frac{\partial u_\phi}{\partial \phi} - u_\theta \tan\theta + \frac{u_r}{r}$$

$$\varepsilon_{\theta\theta} = \frac{\partial u_\theta}{\partial \theta} + \frac{u_r}{r}$$

$$\varepsilon_{\theta\phi} = \frac{1}{2}\left[\frac{\partial u_\phi}{\partial \theta} + \frac{1}{\cos\theta}\frac{\partial u_\theta}{\partial \phi} + u_\phi \tan\theta\right]$$

$$\omega_r = \hat{\mathbf{r}} \cdot (\nabla \times \mathbf{U})$$

Strains and rotations are expressed in terms of derivatives of continuous rotation vector function **W**, defined using bi-cubic spline basis functions. Equivalent to finite-element approach with higher-order elements.

Smoothing or damping in the interpolation of displacements for spatial gradients:

1) Obtain optimal match to displacements while minimizing the model strains
2) Achieve reduced Chi-squared misfit between model and observed displacement field
3) Equivalent to finite-element approach with higher order elements

$$C = \sum_{cells\ ij,kl} \sum (\bar{\dot{e}}_{ij})^T \mathbf{V}_{ij,kl}^{-1} (\bar{\dot{e}}_{kl}) + \sum_{knots\ \ i,j} \sum (v_i - \bar{v}_i^{obs})^T \mathbf{V}_{i,j}^{-1} (\bar{v}_j - \bar{v}_j^{obs})$$

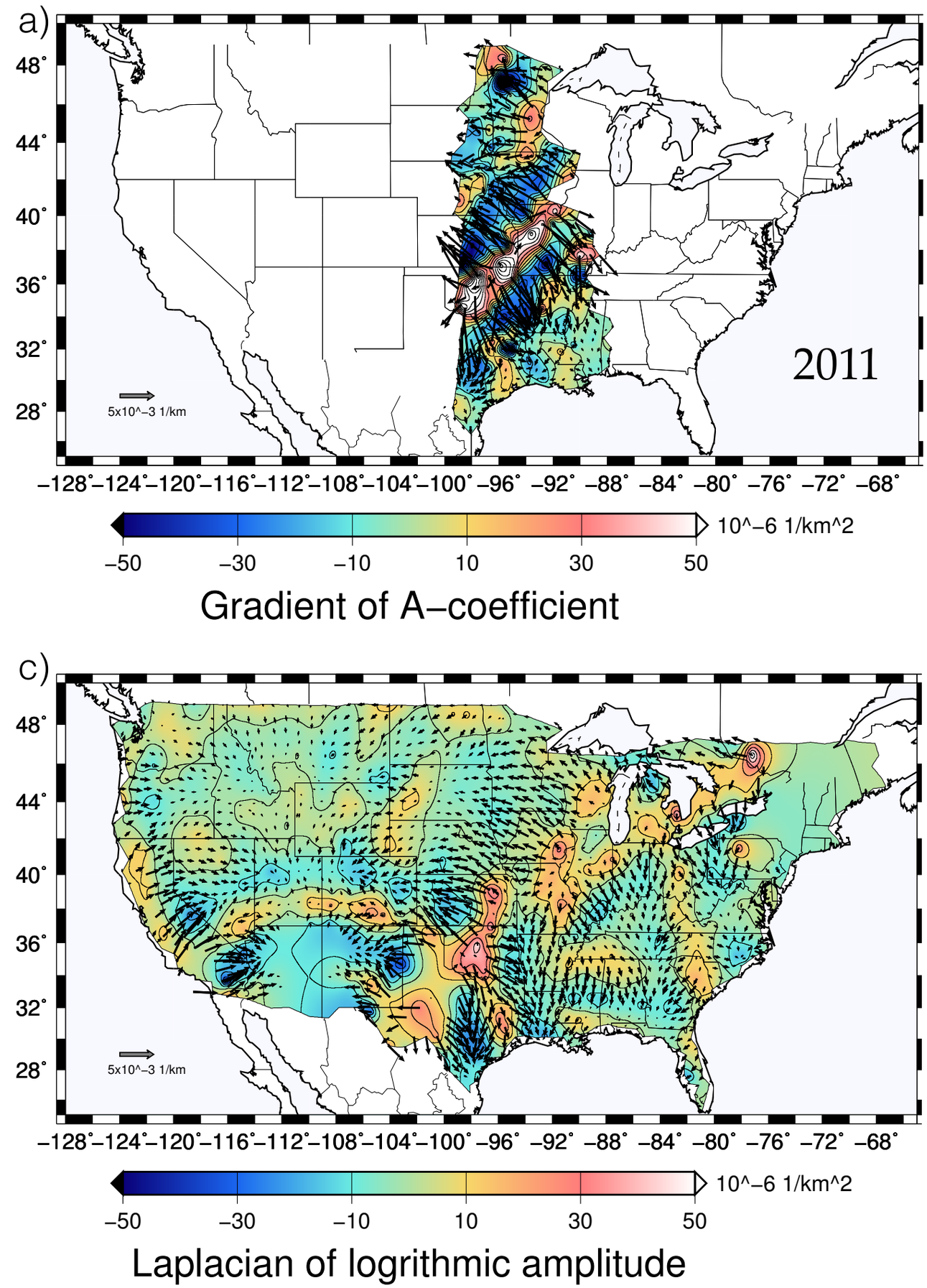

The 60 s Rayleigh wave gradiometry parameters: A-coefficient vectors and gradients for 2011 event obtained from (a) real records (b) synthetics provided by Hejun Zhu at UT Dallas and (c) Global ShakeMovie.

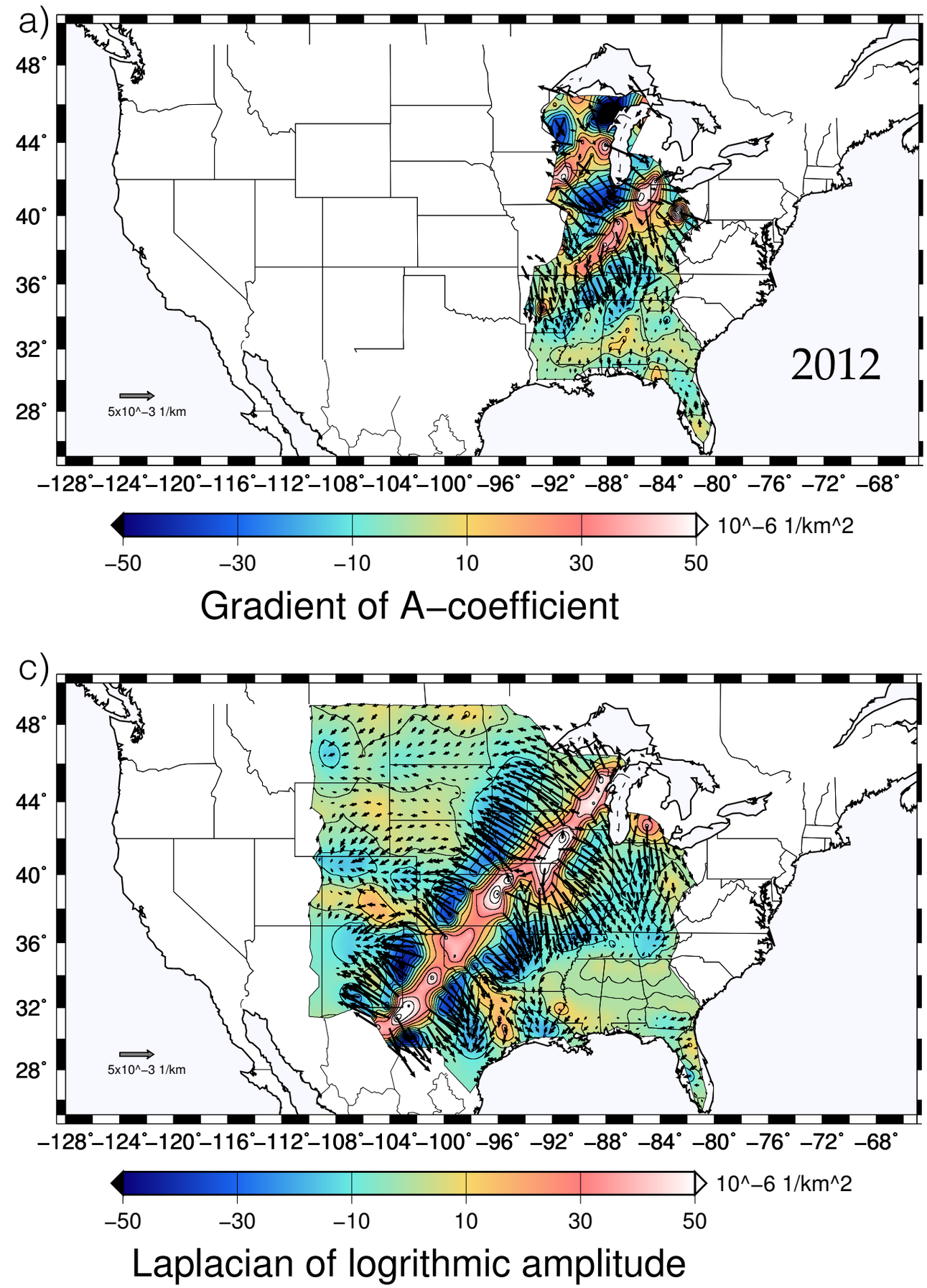

The 60 s Rayleigh wave gradiometry parameters: A-coefficient vectors and gradients for 2012 event obtained from (a) real records (b) synthetics provided by Hejun Zhu at UT Dallas and (c) Global ShakeMovie.

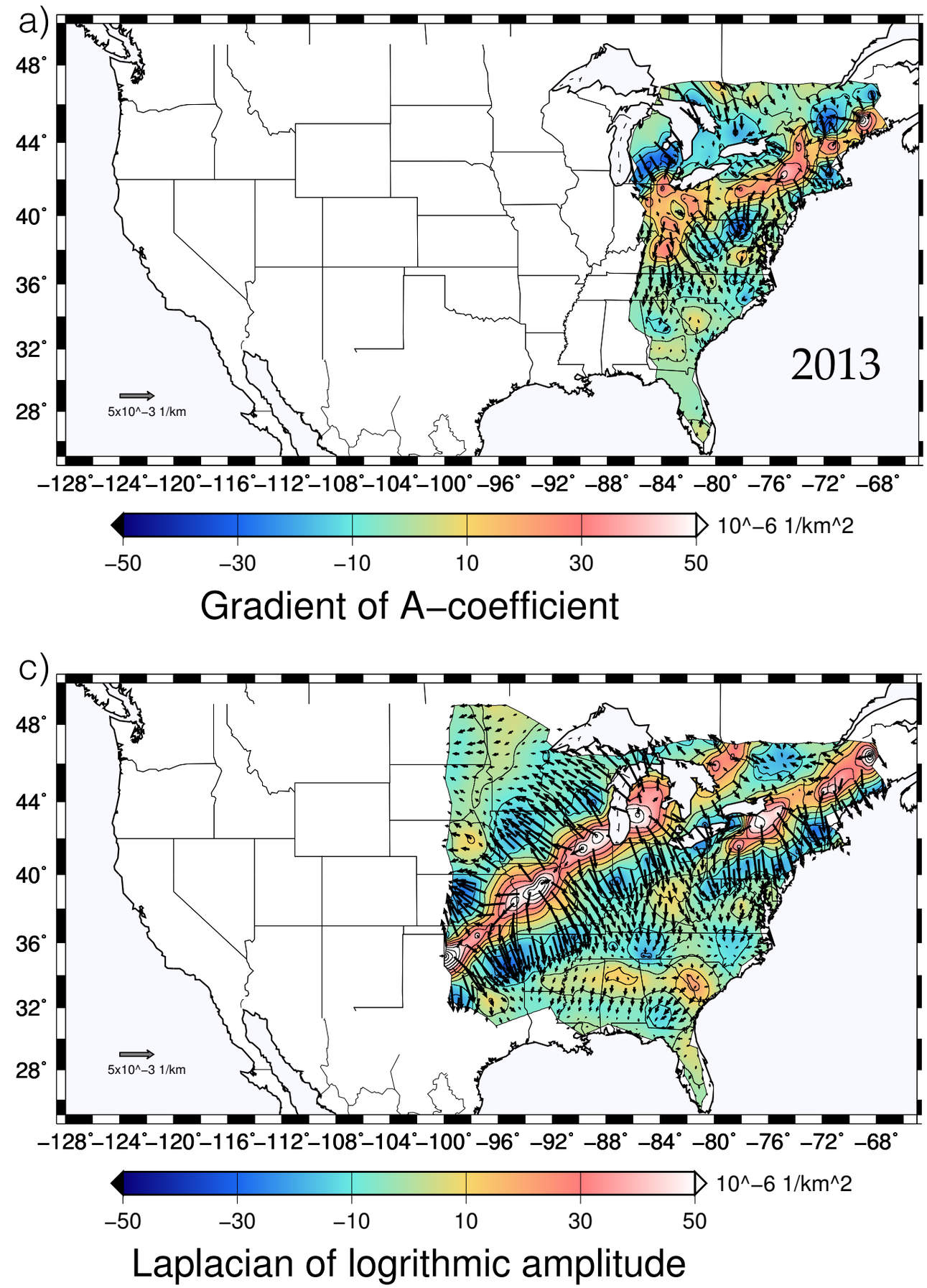

The 60 s Rayleigh wave gradiometry parameters: A-coefficient vectors and gradients for 2013 event obtained from (a) real records (b) synthetics provided by Hejun Zhu at UT Dallas and (c) Global ShakeMovie.

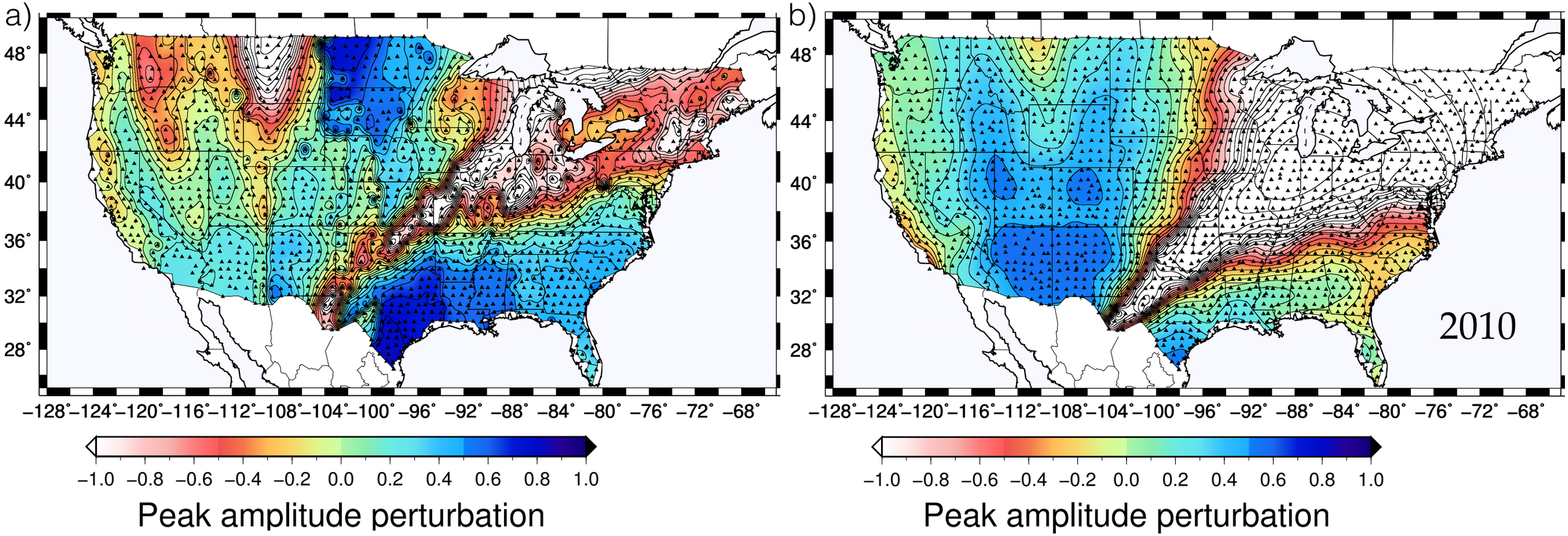

(a) The 60 s Rayleigh wave peak amplitude perturbation combined from six Gulf of California events. Contours are separated by intervals of 0.1.

(b) The same amplitude plot for 2010 event from synthetics provided by Hejun Zhu.

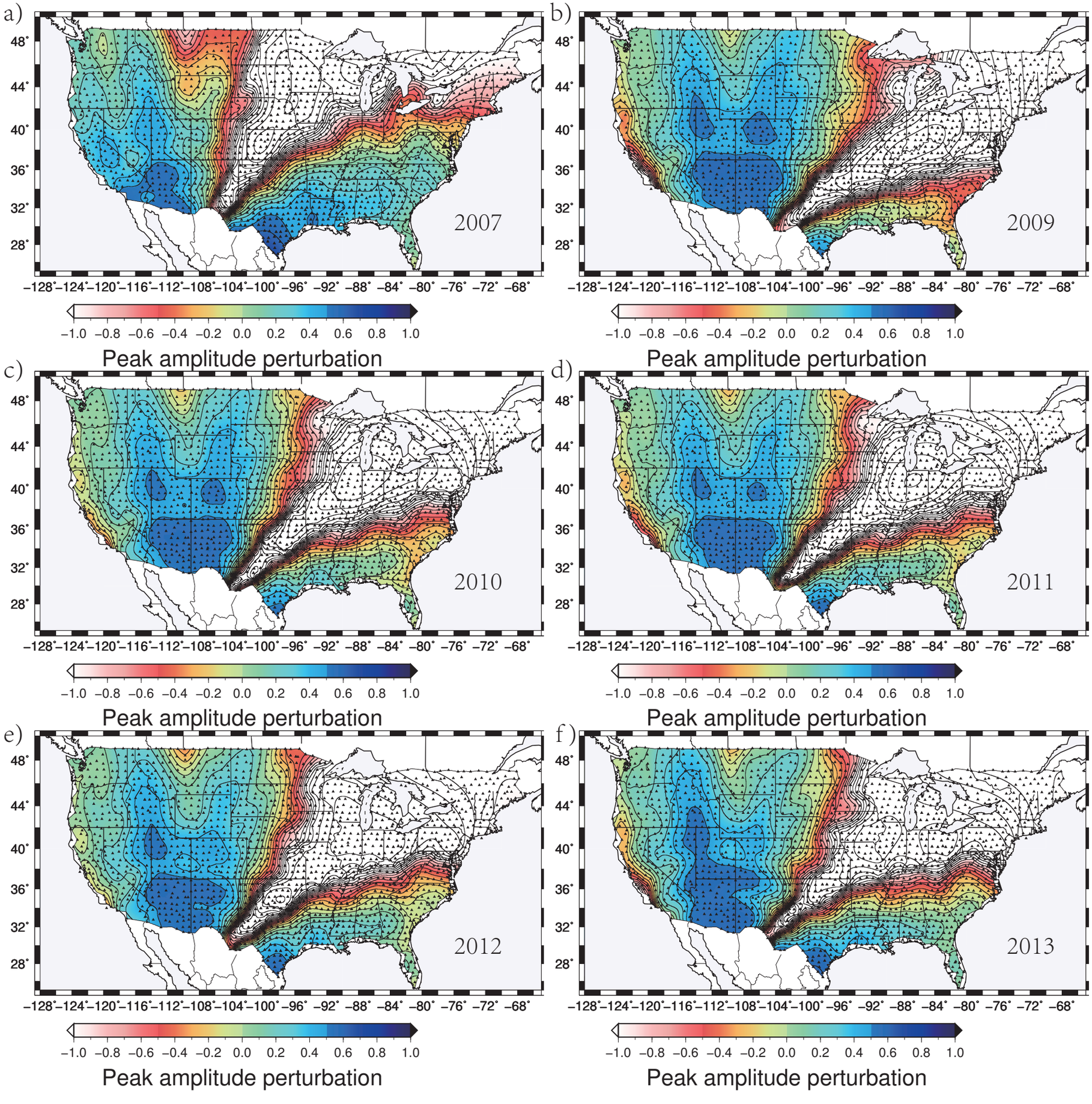
a)
2007
b)
2009
c)
2010
d)
2011
e)
2012
f)
2013
48°
44°
40°
36°
32°
28°
−128° −124° −120° −116° −112° −108° −104° −100° −96° −92° −88° −84° −80° −76° −72° −68°
−1.0 −0.8 −0.6 −0.4 −0.2 0.0 0.2 0.4 0.6 0.8 1.0
Peak amplitude perturbation

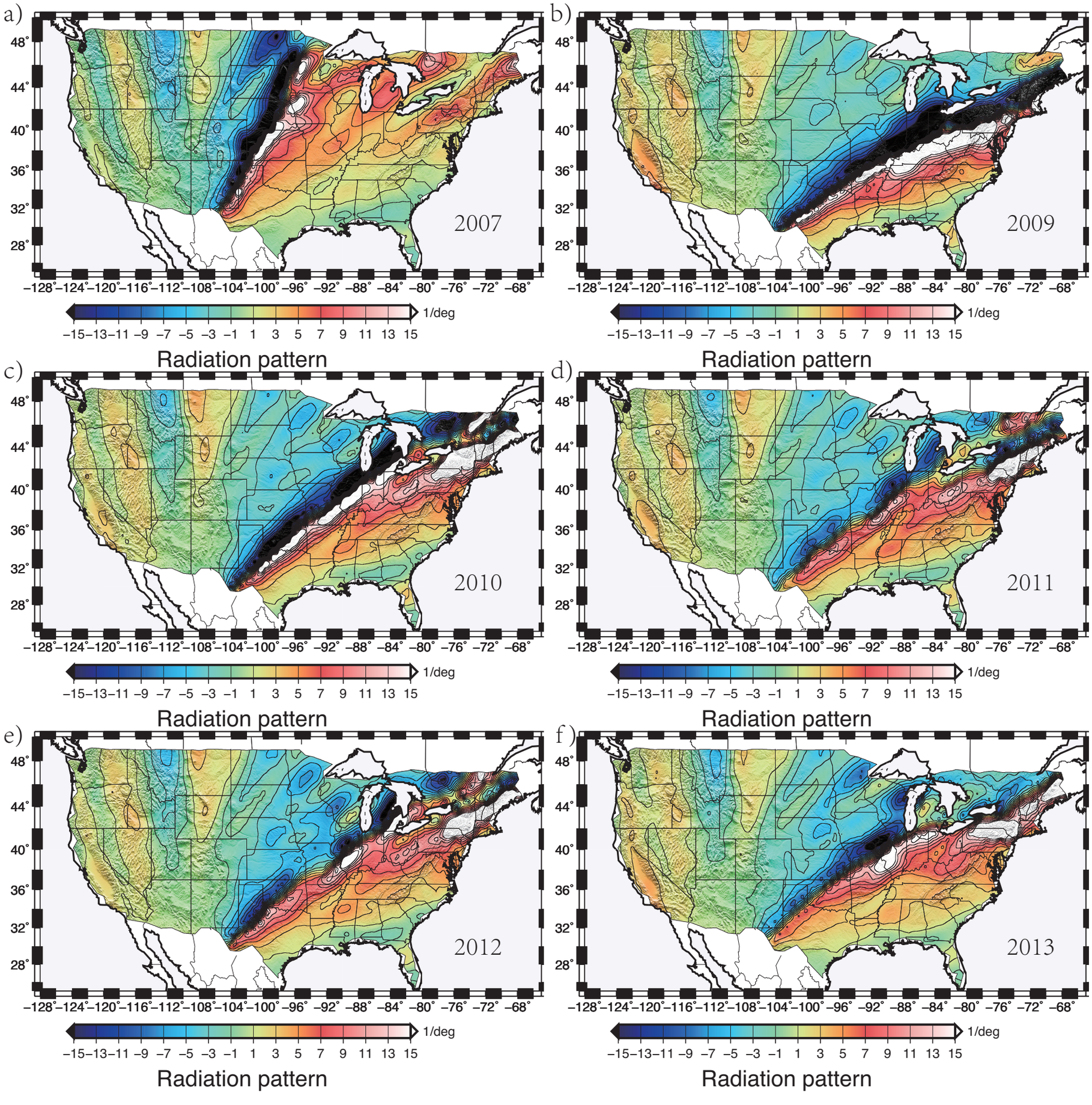
a)
2007
b)
2009
c)
2010
d)
2011
e)
2012
f)
2013
48°
44°
40°
36°
32°
28°
−128° −124° −120° −116° −112° −108° −104° −100° −96° −92° −88° −84° −80° −76° −72° −68°
−15 −13 −11 −9 −7 −5 −3 −1 1 3 5 7 9 11 13 15
1/deg
Radiation pattern

a)

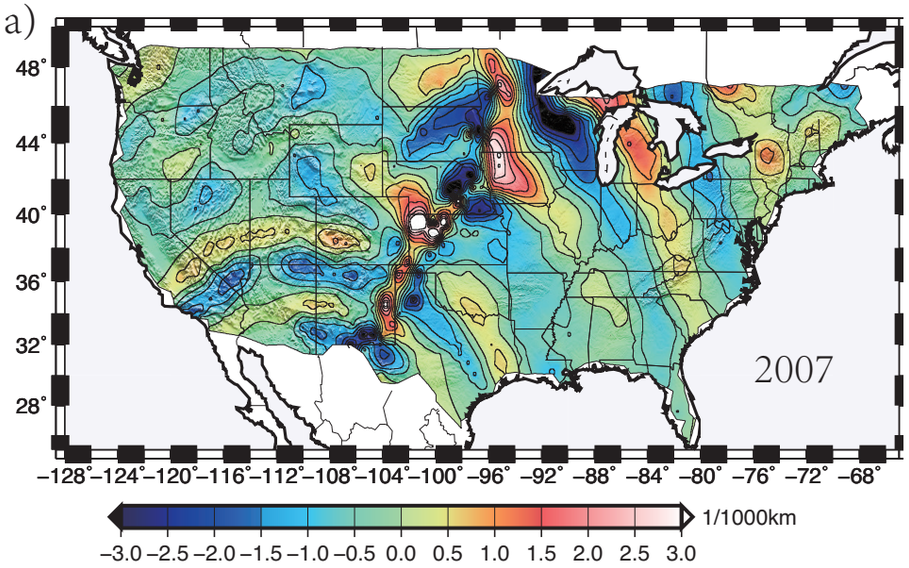

b)

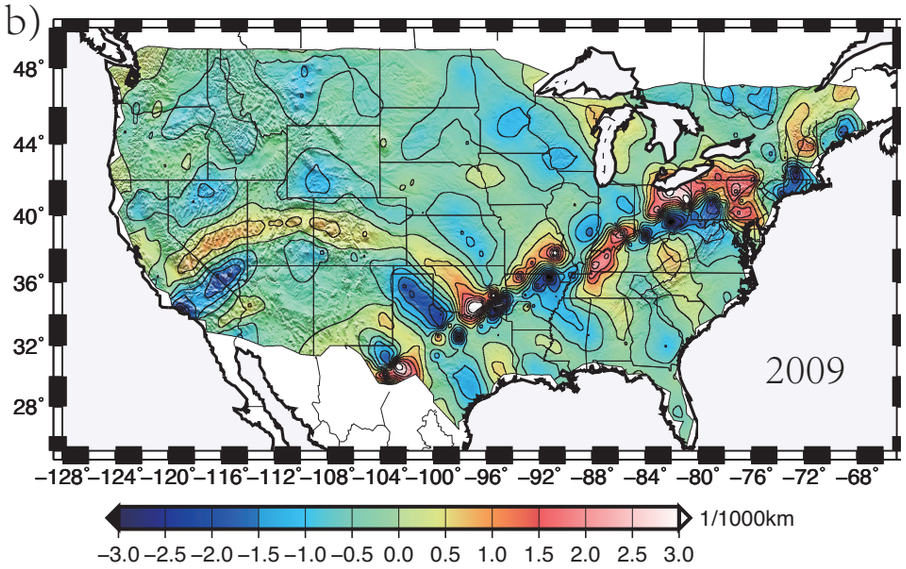

c)

Geometrical spreading

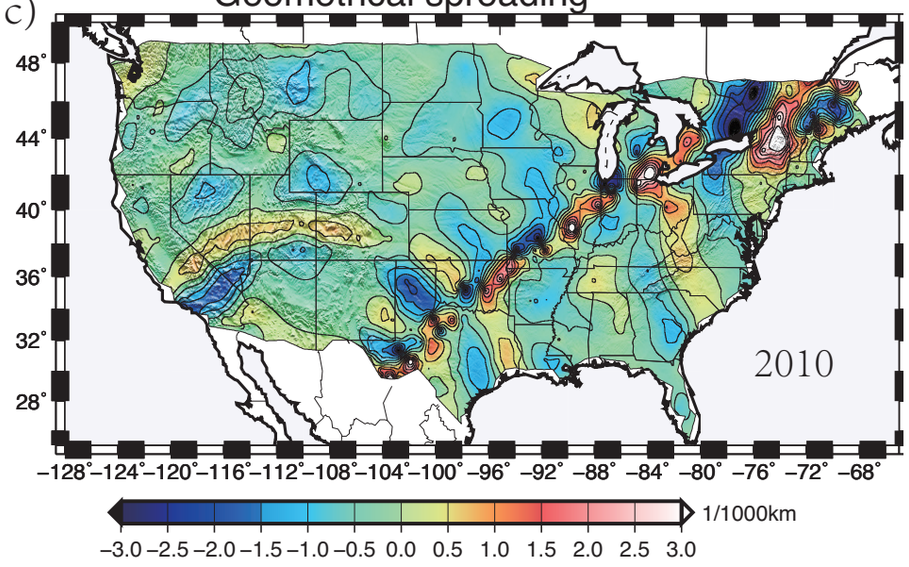

Geometrical spreading

d)

Geometrical spreading

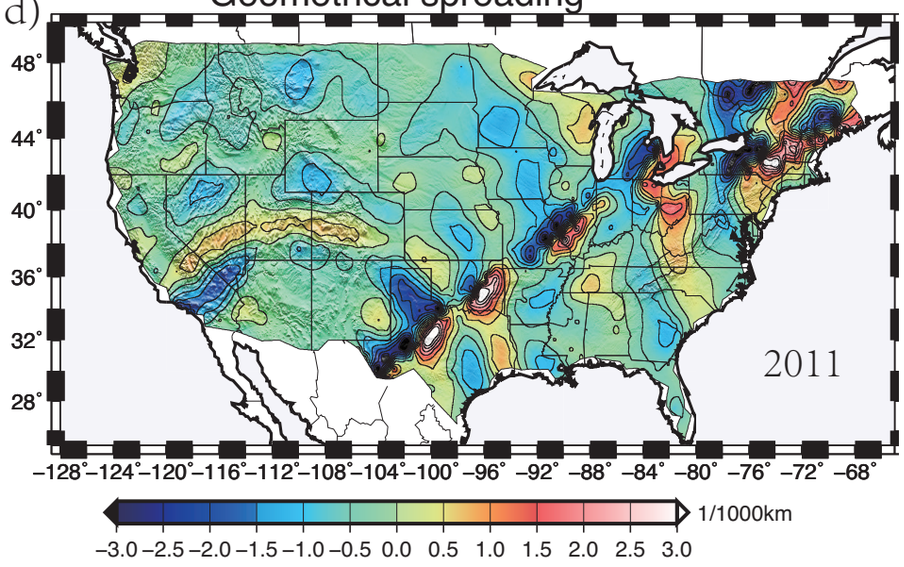

Geometrical spreading

e)

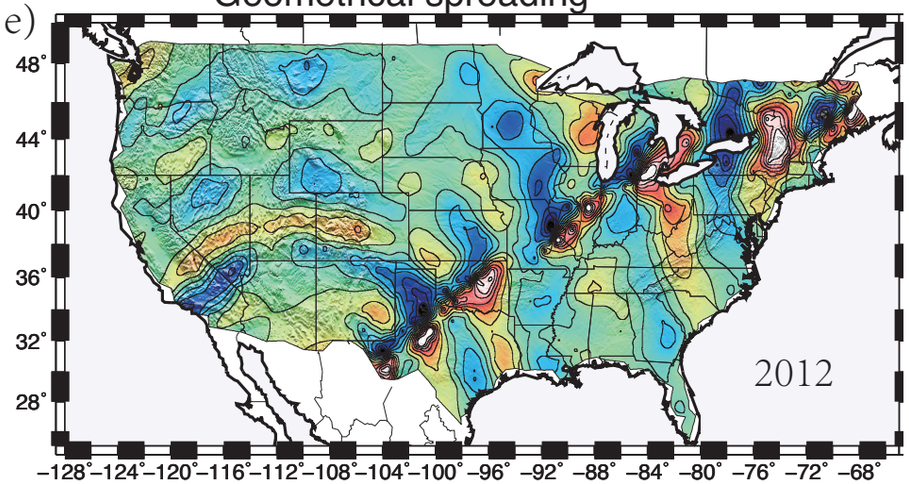

Geometrical spreading

f)

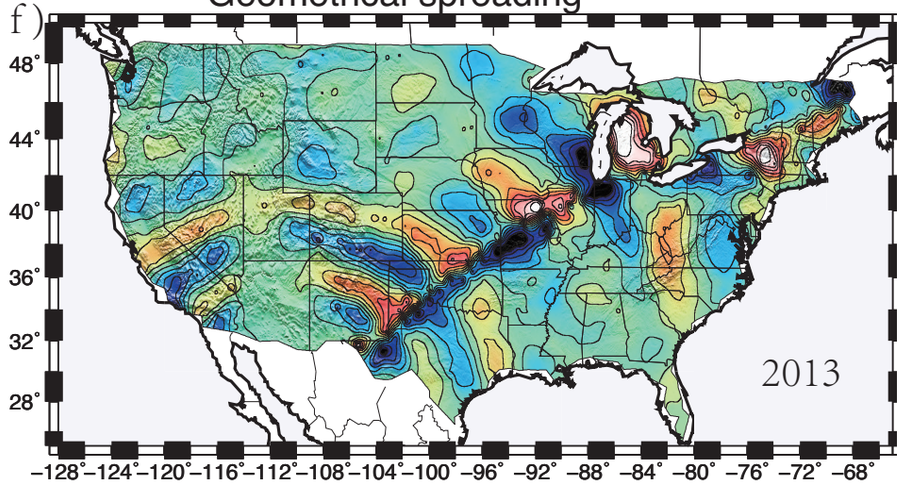

Geometrical spreading

Solved parameters

$$A_x = \frac{\partial G}{\partial x} \cdot \frac{1}{G} \qquad A_y = \frac{\partial G}{\partial y} \cdot \frac{1}{G}$$

$$B_x = -p_x \qquad B_y = -p_y$$

$$p = \sqrt{(B_x^2 + B_y^2)} \qquad A_\theta(\theta) = r(A_x cos\theta - A_y sin\theta)$$

$$\theta = tan^{-1}(\frac{B_x}{B_y}) \qquad A_r(\theta) = A_x sin\theta + A_y cos\theta$$

Helmholtz equation

$$(\Delta + k^2)F(x,y) = 0 \qquad \Delta = \frac{\partial}{\partial x^2} + \frac{\partial}{\partial y^2}$$

$$k^2 = (B \cdot \omega)^2 - A^2 - grad(A)$$

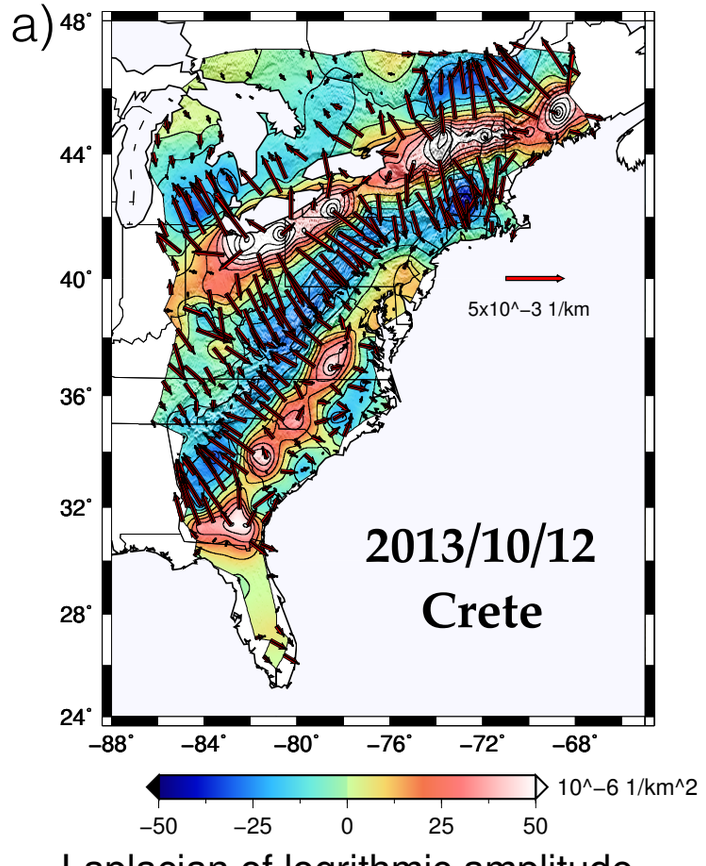

Laplacian of logrithmic amplitude

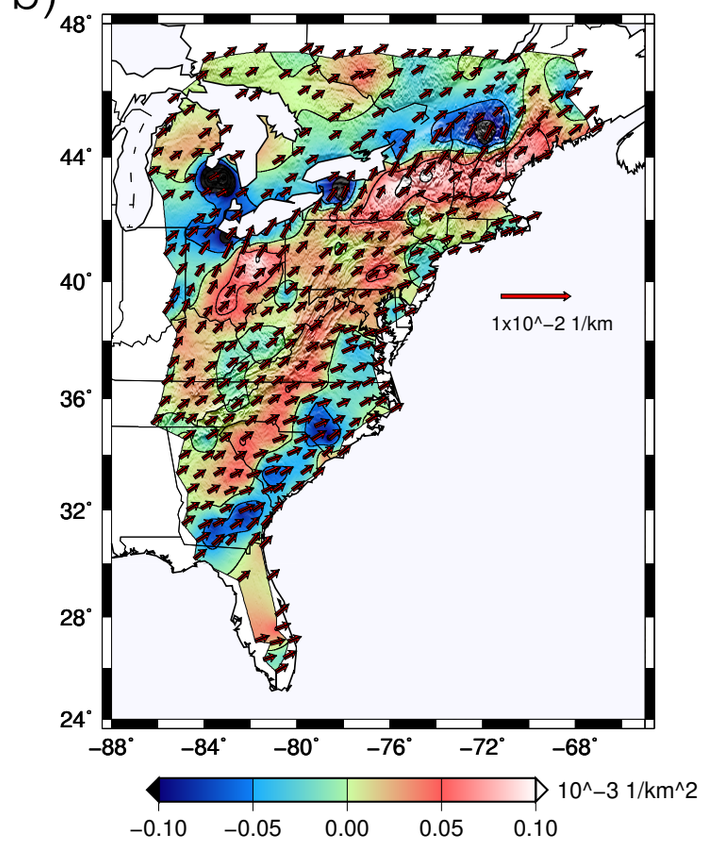

Laplacian of phase

Wave equation solution

$$u(x,y) = G(x,y) f(t - xp_x - yp_y)$$

$$\boxed{\begin{aligned} \frac{\partial u(t,x,y)}{\partial x} &= A_x \cdot u(t,x,y) + B_x \cdot \frac{\partial u(t,x,y)}{\partial t} \\ \frac{\partial u(t,x,y)}{\partial y} &= A_y \cdot u(t,x,y) + B_y \cdot \frac{\partial u(t,x,y)}{\partial t} \end{aligned}}$$